A THERMO-METALLURGICAL MODEL PREDICTING THE STRENGTH OF WELDED JOINTS USING THE FINITE ELEMENT METHOD

Dissertation for the Degree of Ph. D.

MICHIGAN STATE UNIVERSITY

GARY W. KRUTZ

1976

This is to certify that the

thesis entitled

A THERMO-METALLURGICAL MODEL PREDICTING THE STRENGTH OF WELDED JOINTS USING THE FINITE ELEMENT METHOD

presented by

GARY KRUTZ

has been accepted towards fulfillment
of the requirements for

Ph.d. degree in Ag. Engr

Larry J. Segerlind
Major professor

Date 5-20-76

O-7639

ABSTRACT

A THERMO-METALLURGICAL MODEL
PREDICTING THE STRENGTH OF
WELDED JOINTS USING THE
FINITE ELEMENT METHOD

By

Gary W. Krutz

The object of this work was to use finite element analysis in predicting the thermo-history of a welded joint and provide design engineers with a reliable method of optimizing the metallurgical properties of a welded joint.

A finite element computer model was developed and used to determine the time temperature history of a butt weld as related to the heat input. Variables affecting this cooling time include metallurgical constituents, radius of the heat flux, velocity of the arc, and thermal conductivity of molten steel. Thermal conductivity and specific heat were considered as a function of temperature. The latent heat of fusion, and radiation and convection heat transfer were included in the model. A Gaussian distributed heat flux was assumed.

Time-temperature computer results were verified using experimental thermalcouple data available in the literature. Computer determined weld pool size correlated with experimental values.

Joint metallurgy was optimized using a critical cooling time. Fast cooling in the heat affected zone creates hard but brittle metallurgical properties lacking in bend angle strength. Longer cooling times reduce the hardness and increase the bend angle of a weld joint. For this low carbon steel model a definite cooling time, called critical, exists between fast and slow cooling.

Approved Larry J Segerlind
Major Professor

Approved D. R. Heldman
Department Chairman

A THERMO-METALLURGICAL MODEL PREDICTING THE STRENGTH OF WELDED JOINTS USING THE FINITE ELEMENT METHOD

By

Gary W. Krutz

A DISSERTATION

Submitted to
Michigan State University
in partial fulfillment of the requirements
for the degree of

DOCTOR OF PHILOSOPHY

Department of Agricultural Engineering

1976

ACKNOWLEDGMENTS

The author wishes to express his appreciation to Dr. Larry J. Segerlind, whose guidance and helpfulness were indispensable during this study.

In addition, thanks are in order for Sandy Clark for typing this manuscript.

A special dedication of this work is intended for my wife, Barbara, for her continual encouragement throughout this program.

TABLE OF CONTENTS

LIST OF FIGURES

I. Introduction

Welding is probably the most popular manufacturing process used for joining metals in structural applications. It is a common method used in fabricating farm equipment and many times the size of the weld area will govern the size of the components. Because of its wide and flexible use, weld strength has been the concern of designers and researchers who have studied it both analytically and empirically in an effort to maximize the joint strength. This maximization when achieved would reduce the weight of machines, structures, components and save material cost and processing energy.

The goal of this work was to develop a general numerical model of the welding process which is capable of predicting the strength of a weld joint via the metallurgical viewpoint. Since many variables enter the process and this is the first attempt at a particular metallurgical model the study will be limited to low carbon steel. The properties of low carbon steel are not constant but vary from piece to piece as a result of process variations (15).

The problems of distortion, residual stresses, and reduced strength of the material in the joint area are

results of the large amount of heat energy applied at the weld site over a short period of time. This heat gradient at elevated temperatures causes dynamic changes in the weld metallurgy and affects the joint toughness. The finite element method was used to predict the transient thermo-history of a welded composite. The joint strength was predicted from the temperature history.

It is hoped that this method will provide practicing engineers with a technique that will be widely used in weld-joint design.

II. Literature Review

2.1 Past History

The problem of fast cooling rates and high temperatures that change the metallurgy and distort the joint have been concerns of the engineers for years. D. Rosenthal (1,2,3) developed the mathematical theory of heat distribution in welding during the late 1930's. By using the conventional heat transfer differential equation for a Quasi-Stationary State Rosenthal developed equations for point, linear and plane sources of heat. These equations closely approximated actual tests and presented a method of predicting time and rate of cooling with some accuracy for a wide variety of steel thicknesses, ranges of temperature and welding conditions.

$$\frac{\partial^2 T}{\partial x^2} + \frac{\partial^2 T}{\partial y^2} + \frac{\partial^2 T}{\partial z^2} = \rho c \frac{dT}{\partial t}$$ Quasi-Stationary State Eqtn.

Further work on time-temperature relationships was needed because Rosenthal's work was primarily applicable to butt joints and assumed many constant inputs and boundaries.

2.2 Time-Temperature Relationships

Adams (16) took the basic equations of Rosenthal and derived relationships to provide cooling rates and peak-temperatures as a function of geometry, thermal and welding variables. This thermal history is needed to make the metallurgical interpretations in the weld heat affected zone. Using a point heat source Adams developed a three-dimensional conduction model.

$$T^1 - T_o = \frac{8V}{4\pi K\alpha} \frac{EXP[m - \sqrt{m^2 + n^2}]}{\sqrt{m^2 + n^2}}$$

T^1 = steady state temperature at point (X, R)

T_o = initial temperature of the plate

X = distance behind source parallel to movement on axis centerline

α = thermal diffusivity $(\frac{K}{\rho C_p})$

q = rate of heat flow from source

K = thermal conductivity of plate

V = velocity of source

ρ = density of plate

C_p = specific heat of plate

m = $VX/2\alpha$

n = $VR/2\alpha$

R = radial distance (cylindrical coordinates)

For thin plates he predicts heat flow with a two-dimensional steady state temperature distribution given as:

$$T^1 - T_o = \frac{8V}{2\pi Kt} \; e^m \; K_o\sqrt{m^2 + n^2}$$

t = thickness of plate

$K_o(P)$ = modified Bessel function of the second kind and zero order

From these equations he expressed peak-temperature as a function of distance from the fusion zone.

Paley (17) et al. expanded on Adams' work and developed a numerical relationship to provide peak-temperature distributions for submerged-arc welding. They determined that peak temperature, not heating or cooling rates, was the important variable in determining the metallurgy of the heat affected zone (HAZ).

Paley (18) recently used a numerical method (finite differences) to determine the thermal history of welds. This computer program solved the heat flow equation and showed good correlation with experiments in determining the macrostructure of welds. Graphic displays of both the maximum temperature and the moving temperature field in horizontal and vertical planes were some of the output. Computerized plotting of thermal cycles allowed comparison of metallurgy with this numerical technique. He also did an experiment to show that the surface condition (emissivity) of the steel plate had no effect on the shape of isotherms.

Hess (19) did an extensive experimental procedure in determining cooling rates and provides an enormous

amount of data. From his studies he concluded that arc travel speed, arc voltage, and arc current can be conveniently grouped into a single factor called energy input per unit of weld (joules per inch). Then for low carbon steels the only factors affecting weld cooling rates are energy input, plate thickness, plate temperature, and joint geometry.

A study of cooling curves was done by Paschkis (20) by means of electrical analogy. He concluded that the physical properties of steel varied with temperature and more information in this area is needed. Since his study Goldsmith (11) has provided this information needed by Paschkis.

Christensen (49) developed charts to determine weld and HAZ width using basic theory. Roberts (50) studied the relationship between plate size and temperature distribution.

Most of these analytical theories were summarized by Meyers et al. (53) where he states the assumptions which make their usefulness limited. The assumptions are:

1. The material is solid at all times and at all temperatures, no phase changes occur, and is isotropic and homogenous.
2. The thermal conductivity, density, and specific heat are constant with temperature.

3. There are no heat losses at the boundaries, i.e., the piece is insulated.
4. The piece is infinite except in the directions specifically noted.
5. Conditions are steady with time, i.e., in the middle of a long weld, heat input, travel speeds, etc. are steady.
6. The source of heat is concentrated in a zero-volume point, line or area.
7. There is no Joule (I^2R electric) heating.

Because of these limitations researchers of the 1970's have gone to numerical methods which can handle the above seven items.

2.3 Metallurgical aspects

Mahla (4) et al. noted cracking in the base metal was caused by metallurgical changes introduced during the welding process. This cracking results when austenite steel is cooled too rapidly forming brittle martensite. Rates of transformation of austenite can be predicted from Continuous Cooling Transformation Curves (CCT) and the resultant metallurgical properties determined. Therefore the range of properties for a given weld can be predicted if four influencing factors are known:

(1) Rate of heating

(2) Maximum temperature and time at that temperature

(3) Rate of cooling

(4) Composition of the base metal

Mahla's experiments with SAE 1020 steel plates of 1.9 cm thickness or less were entirely free of martensite. He also determined that as the plate size increased from .6 cm to 1.9 cm the cooling rate increased from 10°K per second to 29°K per second respectively. These rates were measured in a range of temperature of 767-870°K.

Dolby and Sanders (5) investigated the metallurgical factors controlling the toughness of the heat affected zone for a range of steels. Dolby's results were similar to Mahla et al. A specimen with the absence of martensite showed the embrittlement to be in the HAZ region where peak temperatures were close to the Ac_3 temperature. With martensite present the regions adjacent to the fusion boundary were the weakest. Strain concentrators existing in the parent metal and HAZ were the only significant variable on toughness for subcritical temperature regions of the HAZ. In their tests refining the HAZ after welding did increase the joint toughness.

Lancaster (6) generalized that the larger the weld pool the coarser the grain where larger grains are associated with poor impact properties. With special additives suitable grain refinement can be achieved.

Stout and Doty (7) define the HAZ in steels as occurring in four distinct areas as shown in Figure 1. Area A is heated slightly above the transformation range causing some of the pearlite to go to austenite. Upon cooling austenite transforms to fine pearlite. The ferrite is not disturbed in this area. In area B during the welding process pearlite goes to austenite and some ferrite is dissolved. Upon cooling pearlite forms in a scattered grain sense. Area C which is closer to the weld pool has complete transformation to austenite. This area is moderately fast cooled limiting ferrite and forming fine pearlite. The area next to the fusion line (area D) has coarser grains than area C being at a higher temperature. Stout and Doty include micrographs that depict the HAZ area and its metallurgical structure in their book.

Henry (8) gives a very good overview of what happens metallurgically during the heating and cooling of the areas around the weld metal. The 1175°K temperature is the beginning point of grain growth. Henry points out that these grown grain structures will not break up into smaller grains unless work is applied or unless the grains undergo a transition. This transition is the cooling below 1175°K where gamma grains form alpha iron resulting in larger alpha grains transforming from larger gamma iron.

The structure of the weld metal is discussed by

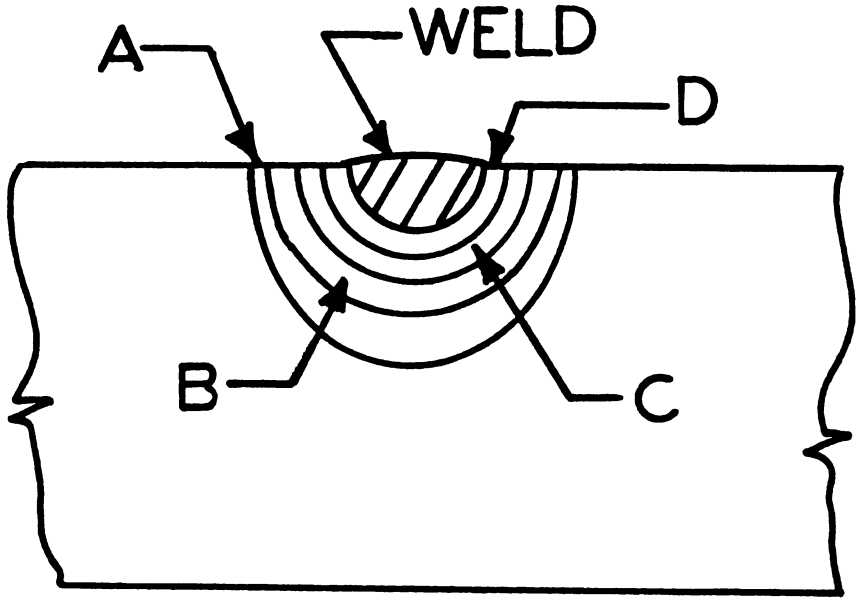

Figure 1. Weld Heat Affected Zones.

Linnert (9). The four common features observed are:

1. Macrostructure columnar growth which follows direction of thermal flow from the weld area.
2. Fine grain size.
3. Substructure contains a large number of dislocations.
4. A Widmanstätten pattern develops.

The properties of the weld metal are dependent on their metallurgical composition which varies greatly with different processes, base metals, and etc. The orientation of grains tends to lower the ductility and toughness.

Inagaki (10) et al. developed monographs to determine cooling time given heat input and plate thickness. Then from CCT curves they concluded existence of a minimum critical cooling time (C_f) which the weld HAZ should cool over to provide the best ferrite-pearlite composition in alloy steels. Using the CCT diagrams they approximated the microstructure hardness at any point in the HAZ.

In researching metallurgy of welding steels material properties are needed to be known and are available in various sources (11, 12, 23, 14, 15).

2.4 Residual Stresses and Deformation

Faukel's book (26) exemplified the nature and

significance of residual stresses and thermal deformation.

Residual stresses are induced whenever a material is non-uniformly plastically deformed. In such an operation the permanent strain produced prevents the elastic component from completely recovering. These deformations may be induced by plastic bending, shot peening, grinding, welding, and other operations.

Distortion is a problem in welding and Iwamura (21) studied the thermal stresses of flame forming. A two-dimensional model was used to determine the stresses via a finite element program. The authors concluded that the model could be expanded to the three-dimensional case (moving point source).

Rybicki et al. (22) developed a method of non-linear stress analysis when the physical properties of a material vary with such items as temperature. He (23) later used the finite element method to evaluate deformation due to welding.

The Welding Institute has conducted some research relative to residual stresses and Dawes (24) explains how and what kind of residual stresses result from welding.

In arc welding, a pool of molten metal is surrounded by a relatively cold solid metal. The peak temperature at the fusion zone is approximately 1775°K. Three mm away this temperature will have dropped to 1175°K

and approximately 100 mm away it will be down to around 575°K. Because the surrounding colder material will restrain local expansion and contraction and the heated portion will go into compression elastically then plastically. Cooling will accompany elastic recovery leaving yield magnitude residual tension stresses in the weld metal. The surrounding material will be balanced by compressive stresses. Dawes states that these residual stresses and strains will not have a significant effect on the ultimate tensile strength of a low carbon steel welded joint because they are highly localized.

Schofield (25) reviewed the many techniques to measure residual stresses.

Masubuchi et al. (28, 29, 48) have a two-dimensional finite element program that calculates thermal stress and distortion of bead-on-plate and butt welds. In their program they include material property temperature dependence and yield criterion and have the ultimate goal of minimizing joint distortion.

The control of residual stresses can be accomplished by many means. Metallurgical annealing or deformation of the metal are a couple of examples. Recently many researchers (21, 22, 23, 24, 25, 28, 57, and 61) have become interested in this problem and are making worthwhile contributions. Comparison of numerical results with actual tests in their research usually fails because of the extreme difficulty in measuring subsurface

residual stresses. Also, restraining weldments, ambient temperature variations, and subsequent loading of the structure can increase or completely decrease these stresses. In the future such problems will be resolved and a more representative residual stress weld model developed. The optimal model will come from the joining of the elastic-plastic (residual stress) models and the thermo-metallurgical model.

2.5 Finite Element Applications

The finite-element method is a mathematical modeling technique from which the solution is obtained numerically (computer applications). The superiority of this method is that it can increase the quality and quantity of results, is fast, accurate and economical as compared to other techniques. It resulted from the need to analyze complicated structures and has spread to other areas of engineering and the sciences. Other advantages that may be incorporated in its application are:

(1) the handling of complicated geometries, loading and support characteristics before and during numerical solving.
(2) the combining of various structures and shapes.
(3) the changing of material characteristics, cross section characteristics and wall thickness from element to element.

Whiteman (30) has compiled a book of Finite Element publications. References (31-47) show that an extensive amount of research has been done in the area of thermal stresses. My goal is to apply this method and determine weld strength. Major hurdles include the varying of material properties with temperature and the determination of temperature as a function of time. The basis of time-dependent finite-element analysis has been proposed by Kohler (58), Zienkiewicz (44, 51) and Singh (52). The thermo-mechanical model has been worked on by researchers such as Friedman (55), Hibbit (56) and Westby (57). Westby gives an excellent detailed matrix analysis of a residual stress model varying yield stress, Young's Modulus and other parameters with temperature.

Lubkin (27, 54) developed a finite-element shell model of a welded joint in his study of car frame vibrations.

III. Theoretical Background

3.1 Introduction

In this section, the finite element model used for the joint strength analysis is developed from the fundamental quasi-stationary state heat transfer equation. The approach adopted is of a more detailed type, so the assumptions being made may be critically examined during the development. The model of the welding process was done in a two part analysis: first, the temperature was determined as a function of location and time; subsequently, all points in the heat-affected zone are checked against the critical cooling time from which revisions to the process are recommended or final data acquired.

There are several boundary conditions and physical phenomena which complicate this non-linear problem. These are discussed here pointing out which ones are essential to the model.

1. The materials are subjected to a wide range of temperatures. All properties were considered as functions of temperature with the exception of density. Figure 2 depicts these

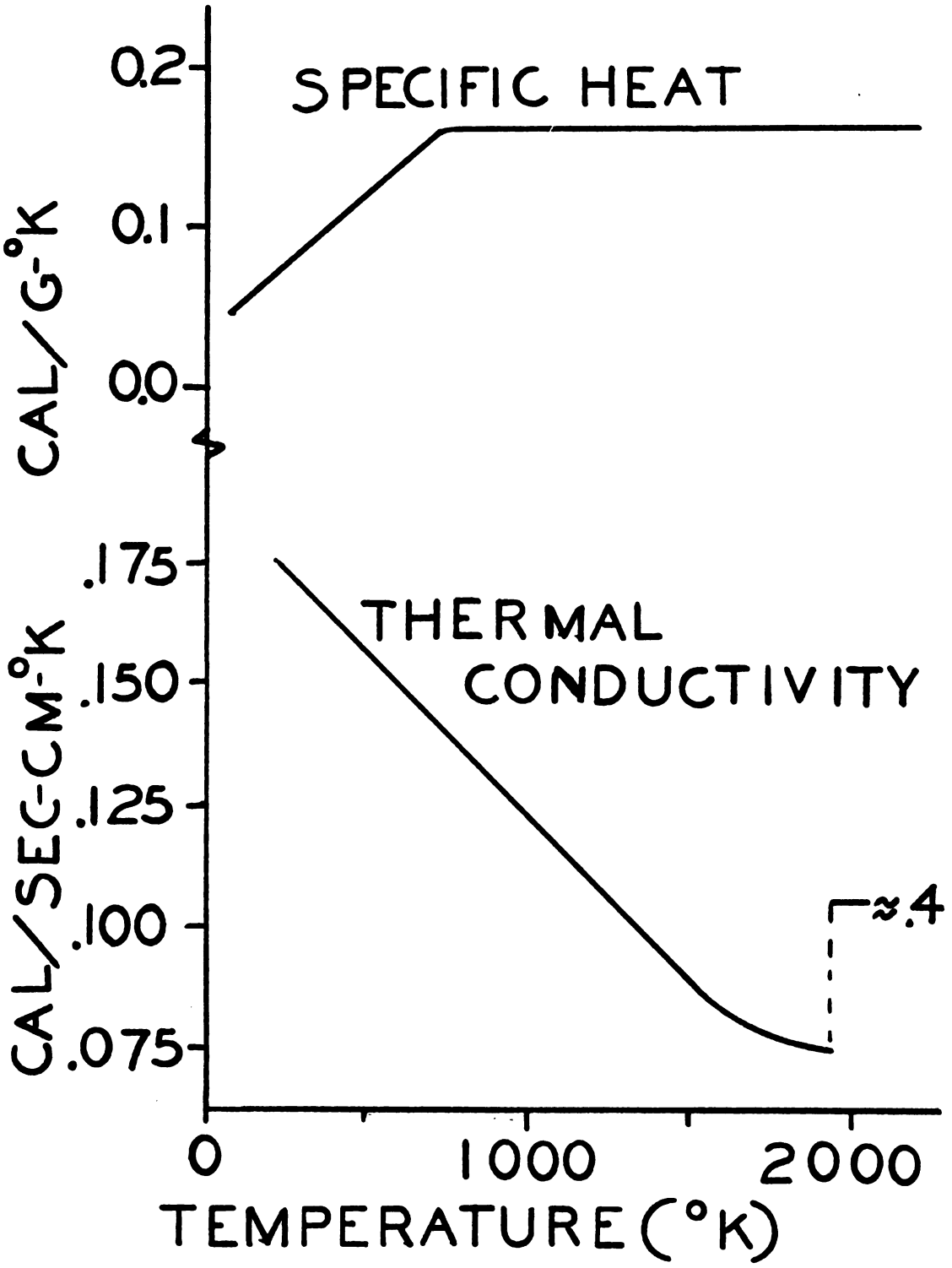

Figure 2. Temperature Dependent Properties of Low-Carbon Steel

properties for Low-Carbon Steel over the temperature range in question. The important properties affected are thermal conductivity and specific heat. It was assumed that the thermal history (i.e. thermal expansion) has little or no effect on the shape of the elements. In actuality the molten and plastic zones deform due to shrinkage and restraints.

2. The phase changes are another important phenomenon affecting this work. The heat of transformation and latent heat of fusion represent a storage of heat during the welding process and subsequently greatly affect the cooling time and microstructure metallurgy. This heat is large enough that it may create favorable recrystallized fine-grained ferrite/pearlite or unfavorable brittle structures. An implicit heat absorption feature to simulate the phase change over a temperature range was included. Most models assumed that the phase change takes place at a specific temperature which is not the case for alloys.

3. Shrinkage distortion and residual stresses are existent and noticeable in the work-piece, but considerable analytical progress must be achieved to provide accurate and meaningful results. All current methods are unable to predict cracking, a common occurrence in many types of welds, and therefore

this model has taken another approach.

4. Input heat flux has been passed over lightly by some researchers who have used voltage times current multiplied by an efficiency factor. A more complete description of the heat flux as a function of position and time will be presented. The addition of filler metals does affect heat input, but will not be added to the finite-element grid because of the difficulty in element modeling.

5. Boundary conditions must account for both radiation (quartic Stefan-Boltzman) and linear Newton convective cooling. No forced convection was assumed and the effects of gas diffusion in the weld pool were not considered. Also, slag formation and its effects were assumed small and negligible because the width of slag is dependent on the process or rod coating and its formation at lower temperatures should have a reduced effect on convection and element conductivity.

6. Weld pool size was determined by the location of the solidus line. The model was assumed two-dimensional and because of symmetry only one half was constructed and analyzed.

The second part is the determination of the critical cooling time factor. Inagaki (10) did a

large amount of experimental work determining a relationship between energy absorbed during a weld joint bend test and the cooling time of the weld joint. It was concluded that the energy absorbed decreased as the cooling time decreased beyond a certain value. Therefore, it was recommended that a minimum critical cooling time (C_f') should be preserved to give maximum joint strength. This C_f' was related empirically to the equivalent carbon content of alloy steels thus providing a guideline for a wide range of materials. Since hardness and tensile strength are related, the critical cooling time becomes an optimum for joint strength seeing multiple loading conditions. The finite element model will be geared to maximize joint strength using the critical cooling time as the optimization criteria.

3.2 Finite Element Formulation of the Welding Process

The predominant mechanism controlling temperature distribution in the welded joint is thermal conduction. Heat conduction in a solid body is expressed three-dimensionally in the following general form:

$$c\rho \frac{\partial T}{\partial t} = \frac{\partial}{\partial x}\left(K\frac{\partial T}{\partial x}\right) + \frac{\partial}{\partial y}\left(K\frac{\partial T}{\partial y}\right) + \frac{\partial}{\partial z}\left(K\frac{\partial T}{\partial z}\right) + Q$$

where T = temperature (K°)

K = thermal conductivity (cal/cm sec °K)

$c\rho$ = volumetric specific heat ($cal/cm^3 °K$)

Q = exchange of heat [convection, radiation, latent heats, and heat flux] ($cal/cm^3 sec$)

When analyzing a two-dimensional body this three-dimensional equation can be modified by deleting the unwanted coordinate direction.

In the finite element method for field problems (heat conduction) a Ritz approximation in variational form replaces the differential equation. The exact solution is then obtained by minimizing this Ritz variational form which also satisfies the boundary conditions. This minimization is obtained by differentiating the variational function and setting it equal to zero. To check that the derivative of the functional equal to zero is a minimum the second derivative is taken and its value must be positive for all ranges of the functions to rule out maximums and points of inflections.

This variational process is covered in various publications (62, 63) which provide greater detailed background.

The heat conduction functional for an individual finite element has been determined by mathematicians and is expressed as:

$$I^e = \int_{V^e} \frac{1}{2} \{T\}^T [B^e]^T [D^e] [B^e] \{T\} dV - \int_{V^e} Q[N^e]\{T\} dV$$

$$+ \int_{S_1^e} q[N^e]\{T\} dS + \int_{S_2^e} \frac{h}{2} \{T\}^T [N^e]^T [N^e] \{T\} dS + \int_{S_2^e} hT_\infty dS$$

$$- \int_{S_2^e} hT_\infty [N^e]\{T\} dS + \left(\int_V \alpha [N^e]^T [N^e] dV\right) \frac{\partial \{T\}}{\partial t}$$

where $\alpha = c\rho$ (c = specific heat, ρ = density) $\left(\frac{cal}{cm^3 \circ K}\right)$

T_∞ = ambient temperature ($^\circ$K)

h = convection coefficient $\left(\frac{watts}{cm^2 \circ K}\right)$

S = surface area (cm^2)

V = volume (cm^3)

e = notation for an element

$[N]$ = shape function of a finite element

$[B] = \left[\frac{\partial N_i}{\partial X_j}\right]$

$[D] = \begin{bmatrix} K_{xx} & 0 \\ 0 & K_{yy} \end{bmatrix} \left(\frac{watts}{cm \circ K}\right)$

Since quantities such as Q, q, T_∞, and h may vary over an element, they are left within the integral.

Again, the solution is obtained by the Ritz Method of minimizing the functional (I) and is expressed as:

$$\frac{dI}{d\{T\}} = \sum_{e=1}^{E} \frac{dI^e}{d\{T\}} = 0$$

When this functional is set equal to zero, the following system of equations results

$$[C]\{\dot{T}\} + [K]\{T\} + \{F\} = 0$$

Contributions from each finite element to this system of equations is:

$$[C^e] = \int_{V^e} \alpha [N^e]^T [N^e] dV = \text{Capacitance Matrix}$$

$$[K^e] = \int_{V^e} [B^e]^T [D^e] [B^e] dV + \int_{S^e} h [N^e]^T [N^e] dS$$

$$= \text{Stiffness Matrix}$$

$$\{F^e\} = - \int_{V^e} Q [N^e]^T dV + \int_{S^e} q [N^e]^T dS - \int_{S^e} h T_\infty [N^e]^T dS$$

$$= \text{Force Vector}$$

This system of equations includes the element of time. A solution can be achieved by using an implicit Crank-Nicolson Method which yields:

$$([K] + \frac{2}{\Delta t}[C])\{T_1\} = (\frac{2}{\Delta t}[C] - [K])\{T_0\} - 2(\frac{\{F_1\}+\{F_0\}}{2})$$

where subscripted 1's are values at time $t + \Delta t$ and subscripted 0's are values at the initial time t

The values of {T} and {F} are being evaluated at the mid-point of the time interval.

This Crank-Nicolson Method can have solutions that either decay steadily or oscillate in a stable state. When this method is implemented using Finite Differences a required maximum time interval will give stability to the numerical solution. An attempt will be made to use Westby's (69) Finite Difference guidelines regulating the time interval to assure stability. This time interval regulates the number of iterations (calculations) necessary to solve the system of equations and therefore its size must be small enough to minimize instability and large enough to save on computer time. Westby's equation:

$$\Delta t \leq \frac{1}{\frac{2K}{\rho c}\left(\frac{1}{\Delta x^2} + \frac{1}{\Delta y^2}\right)}$$

Δx and Δy are lengths in the finite difference method, and this equation will be considered as a guide in this finite element solution.

Also, the finite element used to model the body must be of an order one less than the governing differential equation. In this two-dimensional transient heat transfer quasi-stationary state equation the order needed is one. Therefore, linear elements may be used to model the weld joint and for the two-dimensional case

triangular elements are the basic requirement. Higher order elements can be used to increase accuracy but they also increase roundoff error and computational time.

The finite element method is a numerical approximation of the true solution. Therefore some error can exist. This error has been expressed as (63):

$$e = A\, h^b$$

where A is an arbitrary constant dependent on the element used

b is the order of the element

h is an element length

From this expression some relative generalization can be discussed on reducing the error. Error reduction can be accomplished by either decreasing the element size or increasing the element order. Both are expensive because they increase computational time. Therefore, some happy medium has to be obtained to assure accuracy. The rule is to refine the mesh in high gradient regions. This grid then relies heavily on engineering judgment.

3.3 Triangular Elements

The two-dimensional simplex element (triangle) meets the requirements for modeling this heat conduction

problem and keeps computation time to a minimum. The shape functions for this element are presented in this section along with other matrix properties that contribute to the system of equations being solved. Figure 3 is a graphical representation of this triangular element where coordinates at the nodes are X_i, Y_i, X_j, Y_j, X_k, Y_k and the values of the temperatures at the nodes designated as T_i, T_j and T_k. Segerlind (62) develops these and other elements in considerable detail.

The temperature of an element (T^e) can be related to node temperature and the element shape.

$$T^e = N_i T_i + N_j T_j + N_k T_k$$

In this relationship there are three shape functions (N_i, N_j, N_k), one for each node.

N_i (shape function at node i) =

$$\frac{1}{2A} [a_i + b_i x + c_i y]$$

where: A = area of the triangle

$a_i = X_j Y_k - X_k Y_j$ (a function of the coordinates)

$b_i = Y_j - Y_k$

$c_i = X_k - X_j$

$$N_j = \frac{1}{2A} [a_j + b_j X + c_j Y]$$

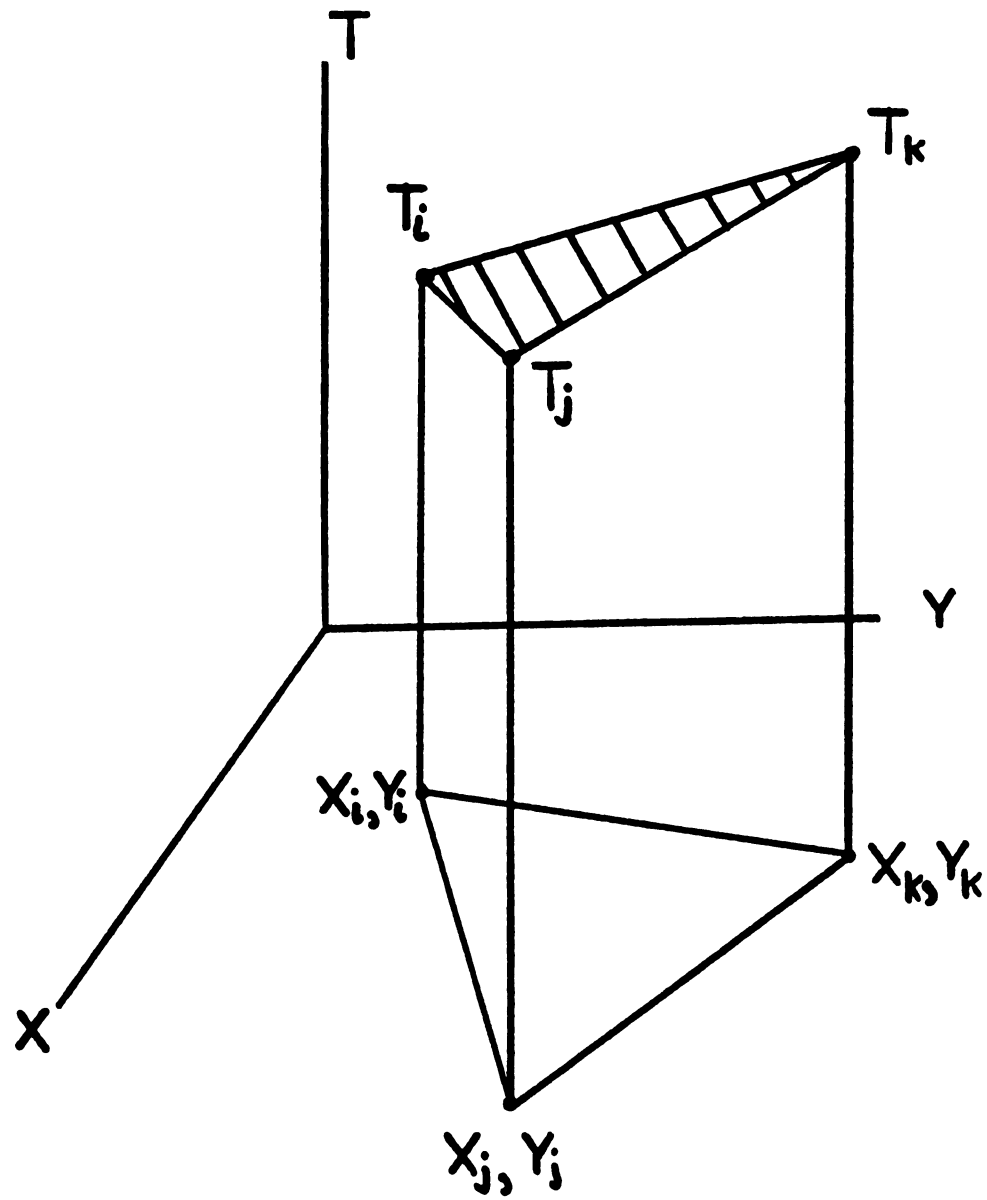

Figure 3. The Two-Dimensional Simplex Element (Triangular Element)

where: $a_j = X_k Y_i - Y_k X_i$

$b_j = Y_k - Y_i$

$c_j = X_i - Y_k$

and $N_k = \frac{1}{2A} [a_k + b_k X + c_k Y]$

where: $a_k = X_i Y_j - X_j Y_i$

$b_k = Y_i - Y_j$

$c_k = X_j - X_i$

The $[B^e]$ is defined for triangular elements as:

$$[B^e] = \begin{bmatrix} \frac{\partial N_i^e}{\partial X} & \frac{\partial N_j^e}{\partial X} & \frac{\partial N_k^e}{\partial X} \\ \frac{\partial N_i^e}{\partial Y} & \frac{\partial N_j^e}{\partial Y} & \frac{\partial N_k^e}{\partial Y} \end{bmatrix}$$

this reduces to

$$[B^e] = \frac{1}{2A} \begin{bmatrix} b_i & b_j & b_k \\ c_i & c_j & c_k \end{bmatrix}$$

and is called the gradient matrix.

These terms can be determined from actual coordinate values resulting in a numerical $[B^e]$. The matrix [N] as it is used in the element equation is:

$$[N^e] = [N_i{}^e \; N_j{}^e \; N_k{}^e]$$

Expanding the element equation in terms of shape functions and node temperatures

$$[T^e] = [N_i{}^e \; N_j{}^e \; N_k{}^e] \begin{Bmatrix} T_i \\ T_j \\ T_k \end{Bmatrix} = [N^e]\{T\}$$

The first term of the $[K^e]$ can be determined by substituting triangular element gradient matrix values in to the volume integral which gives:

$$\int_V [B]^T[D][B]dV = \int_V \frac{1}{4A^2} \begin{bmatrix} b_i & c_i \\ b_j & c_j \\ b_k & c_k \end{bmatrix} \begin{bmatrix} K_{xx} & 0 \\ 0 & K_{yy} \end{bmatrix} \begin{bmatrix} b_i & b_j & b_k \\ c_i & c_j & c_k \end{bmatrix} \quad dV$$

Assuming a unit thickness the coefficients of $[K^e]$ after integration become:

$$K_{Lm} = \frac{K_{xx}}{4A} [b_{Lm}] + \frac{K_{yy}}{4A} [c_{Lm}] \text{ where } L = 1,2,3;\ m = 1,2,3$$

The other terms of the $[K^e]$, $[C^e]$ and $\{F^e\}$ can be determined using various methods and are given as:

$$\int_{L_{ij}} h[N]^T[N]dS = \frac{h\, L_{ij}}{6} \begin{bmatrix} 2 & 1 & 0 \\ 1 & 2 & 0 \\ 0 & 0 & 0 \end{bmatrix}$$

L_{ij} = designates a specific side of the triangle

$$\int_{L_{jk}} h[N]^T[N]dS = \frac{h\ L_{ki}}{6} \begin{bmatrix} 0 & 0 & 0 \\ 0 & 2 & 1 \\ 0 & 1 & 2 \end{bmatrix}$$

and

$$\int_{L_{ki}} h[N]^T[N]dS = \frac{h\ L_{ki}}{6} \begin{bmatrix} 2 & 0 & 1 \\ 0 & 0 & 0 \\ 1 & 0 & 2 \end{bmatrix}$$

Some integrals are evaluated using area coordinates and the results are:

$$Q \int_V [N]^T dV = \frac{QV}{3} \begin{Bmatrix} 1 \\ 1 \\ 1 \end{Bmatrix}$$

$$q \int_S [N]^T dS = \frac{q\ L_{ij}}{2} \begin{Bmatrix} 1 \\ 1 \\ 0 \end{Bmatrix} \text{ or } \frac{q\ L_{jk}}{2} \begin{Bmatrix} 0 \\ 1 \\ 1 \end{Bmatrix}$$

$$\text{or } \frac{q\ L_{ki}}{2} \begin{Bmatrix} 1 \\ 0 \\ 1 \end{Bmatrix}$$

$h\ T_\infty \int_S [N]^T dS$ yields similar values as $q \int_S [N]^T dS$ by replacing q by $h\ T_\infty$.

$$[C^e] = \int_V \alpha[N]^T[N]dV = \frac{c\rho}{12} \begin{bmatrix} 2 & 1 & 1 \\ 1 & 2 & 1 \\ 1 & 1 & 2 \end{bmatrix}$$

In summary the shape of the triangle and its coordinates give numerical values for the general matrices of the Crank-Nicolson approximation. If q, Q, Δt, K_{xx}, K_{yy}, h, and T_∞ are known the only unknown for an element is the temperature at the nodes. For a complex system modeled by triangular elements the minimized variational function is the sum of the contributions from each element. This results in the large system of equations which are solved for the temperature at each node. Many numerical solution techniques are available and some are presented by Segerlind (62).

3.4 Temperature Dependent Properties

The model of a typical butt weld joint is shown in Figure 4. Symmetry of this joint allows the discretization of the body to include only 1/2 of the geometry. In this model smaller triangular elements are used in the high temperature gradient areas where accuracy is important.

Certain variables in the system of equations are temperature dependent or vary with position. These are thermal conductivity, radiation, heat flux, specific heat, and latent heats. The implementation of these temperature and position dependent variables is a significant contribution to the model but each does increase

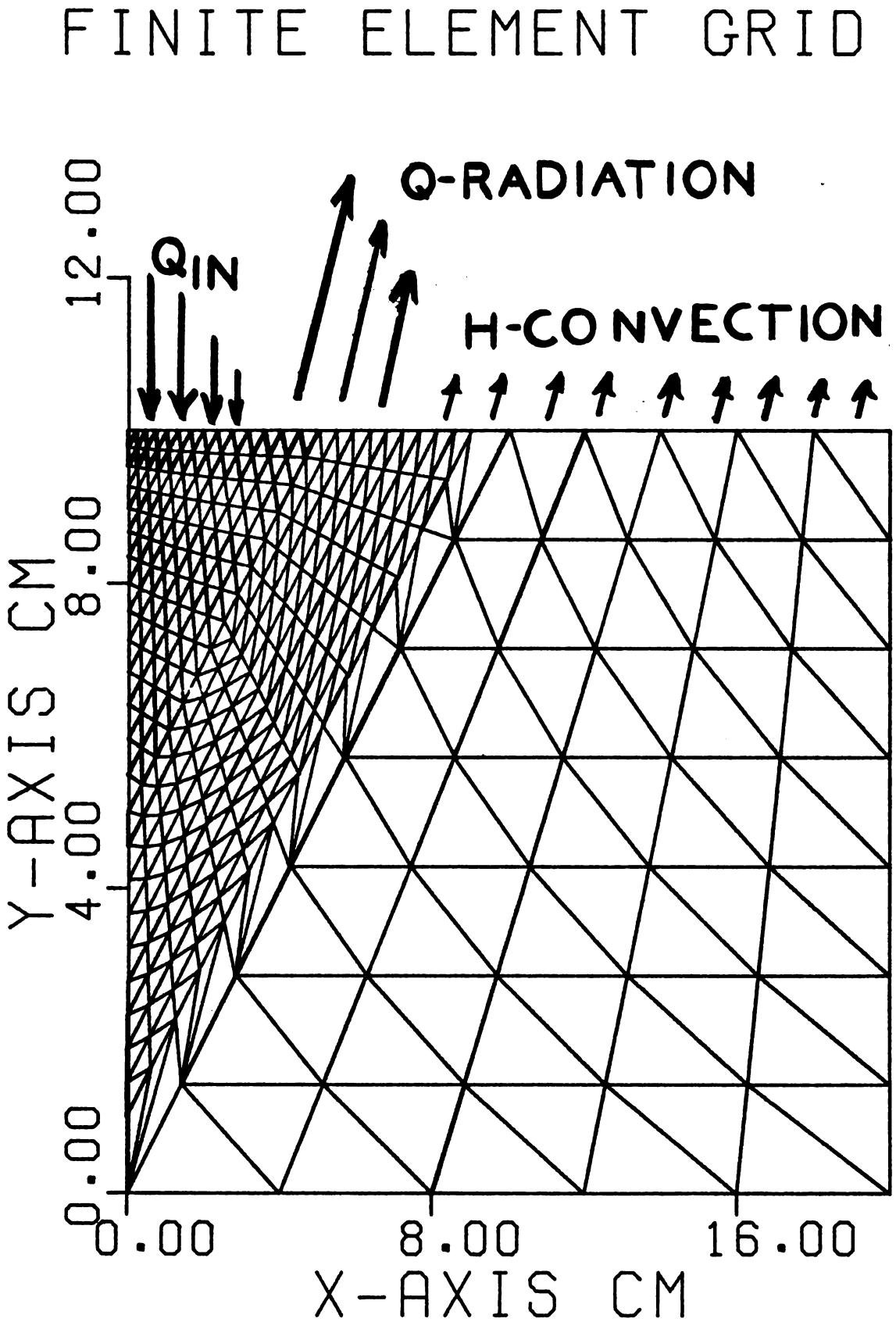

Figure 4. Triangular Element Weld Joint Model

the solution computational time.

For many materials such as low carbon steels varying thermal conductivity linearly with temperature provides a good approximation. This variation can be written as:

$$K_A^e = K_0^e + K_1^e T$$

where K_0^e and K_1^e are constants for an element. If the material was homogenous K_0 and K_1 would be constant for the entire body. Values for K_0 and K_1 are determined from Figure 2. The temperature variation is linear within a triangular element, therefore, a convenient representation of T is to use the arithmetic average of the node temperatures. The following equation results:

$$K_A^e = K_0^e + K_1^e \left(\frac{T_i + T_j + T_k}{3}\right)$$

Now, using thermal conductivity as a function of temperature the process of minimizing the variational form will yield another term in the global stiffness matrix [K]. The variational term that includes thermal conductivity is:

$$I = \int_{V^e} \frac{1}{2}\{T\}^T[B^e]^T[D][B^e]\{T\}dV + \ldots$$ others not necessary for evaluation at this time

Minimizing for temperature dependent thermal conductivity results in:

$$\frac{dI}{d\{T\}} = 0 = \frac{1}{2}\frac{d}{d\{T\}} \int_{V^e} \{T\}^T[B^e]^T[D][B^e]\{T\}dV +$$

$$\frac{1}{2}\frac{dK_A^e}{d\{T\}} \int_{V^e} \{T\}^T[B^e]^T[B^e]\{T\}dV$$

Differentiation of matrix equations yields a standard form

$$\frac{d}{d\{T\}}\left(\{T\}^T[A]\{T\}\right) = 2\,[A]\{T\}$$

Using this the first term becomes

$$\frac{1}{2}\int_{V^e} 2[B^e]^T[D][B^e]\{T\}dV$$

The derivative K_A^e with respect to $\{T\}$ is:

$$\frac{d\,K_A^e}{d\{T\}} = \frac{K_1^e}{3}\begin{Bmatrix}1\\1\\1\end{Bmatrix} .$$

Substituting it into the second term of the minimized variational form that term becomes:

$$\frac{K_i^e}{6} \int_V [T_B]^T [B^e]^T [B^e] \{T\} dV$$

where $[T_B]^T$ is the 3x3 matrix

$$[T_B]^T = \begin{bmatrix} T_i & T_j & T_k \\ T_i & T_j & T_k \\ T_i & T_j & T_k \end{bmatrix}$$

expressing these two terms in matrix form

$$[K_C^e]\{T\} + \frac{1}{6}[T_B]^T [K_B^e]\{T\}$$

or

$$([K_C^e] + \frac{1}{6}[T_B]^T [K_B^e])\{T\}$$

The stiffness matrix $[K^{(e)}]$ is:

$$[K^e] = [K_C^e] + \frac{1}{6}[T_B]^T [K_B^e]$$

when thermal conductivity is a function of temperature. The matrix $[K_C]$ is

$$[K_C] = [B]^T \begin{bmatrix} K_o + K_1 \left(\frac{T_i+T_j+T_k}{3}\right) & 0 \\ 0 & K_o + K_1 \left(\frac{T_i+T_j+T_k}{3}\right) \end{bmatrix} [B]$$

While $[K_B]$ is:

$$[K_B] = [B]^T \begin{bmatrix} K_1 & 0 \\ 0 & K_1 \end{bmatrix} [B]$$

The second term in $[K^e]$ is not a symmetric matrix and, therefore, cannot be combined with $[K_C{}^e]$. This expression for $[K^e]$ must then be substituted back into the matrix form

$$[C]\{\dot{T}\} + [K]\{T\} + \{F\} = 0$$

when thermal conductivity varies with temperature.

3.5 Radiation Boundary Condition

In the weld pool vicinity heat is radiated to the surrounding environment because of the high difference in surface and ambient temperatures. This radiation must be accounted for. The variational function contributing only to radiation is (53):

$$I_r = \sigma\varepsilon \left(\frac{1}{5} T_1^5 - T_{1\infty}{}^4 T_1\right)$$

Taking the derivative of this function results in

$$q_{radiation} = \frac{dI_r}{dT_1} = \sigma\varepsilon \left(T_1^4 - T_{1\infty}{}^4\right)$$

When setting this equal to zero we see that one term can be added on to the global stiffness matrix [K] and the other term is added to the force vector $\{F\}$. Factoring out a $\{T_1\}$ from the first term gives the following form

$$\frac{dI_r}{d\{T\}} = [\sigma\varepsilon T_1^3]\{T_1\} - \sigma\varepsilon T_{1\infty}^4 = 0$$

or sometimes this is shown in the matrix form

$$[R]\{T_1\} - \{r\} = 0$$

where:

σ = Steftan Boltzmann constant = $5.672 \times 10^{-12} \frac{watt}{cm^2 \circ K^4}$

ε = emissivity

T_1 = absolute temperature (°K)

[R] = is the addition to the stiffness matrix [K]

{r} = is the addition to the force vector {F}

Again using area coordinates, radiation from one side of a triangular finite element may be expressed as:

$$\frac{\sigma\varepsilon T_1^3 L_{ij}}{6} \begin{bmatrix} 2 & 1 & 0 \\ 1 & 2 & 0 \\ 0 & 0 & 0 \end{bmatrix} \quad \text{where } T_1^3 \text{ is } \left(\frac{T_i + T_j}{2}\right)^3$$

or

$$\frac{\sigma\varepsilon T_1^3 L_{ij}}{6} \begin{bmatrix} 0 & 0 & 0 \\ 0 & 2 & 1 \\ 0 & 1 & 2 \end{bmatrix} \quad \text{where } T_1^3 \text{ is } \left(\frac{T_j + T_k}{2}\right)^3$$

or

$$\frac{\sigma\varepsilon T_1^{\,3} L_{ki}}{6} \begin{bmatrix} 2 & 0 & 1 \\ 0 & 0 & 0 \\ 1 & 0 & 2 \end{bmatrix} \quad \text{where } T_1^3 = \left(\frac{T_k + T_i}{2}\right)^3$$

Similarly the values affecting the force matrix when used with triangular elements may be expressed as:

$$\frac{\sigma\varepsilon T_{1\infty}^{\,4} L_{ij}}{2} \begin{Bmatrix} 1 \\ 1 \\ 0 \end{Bmatrix}$$

or

$$\frac{\sigma\varepsilon T_{1\infty}^{\,4} L_{jk}}{2} \begin{Bmatrix} 0 \\ 1 \\ 1 \end{Bmatrix}$$

or $$\frac{\sigma\varepsilon T_{1\infty}^{\,4} L_{ki}}{2} \begin{Bmatrix} 1 \\ 0 \\ 1 \end{Bmatrix}$$

where $T_{1\infty}$ is the ambient temperature assumed to be constant over the side. Comini (44) et al. have presented an alternative approach where $\sigma\varepsilon T_1^3$ is replaced by $\sigma\varepsilon(T^2 + T_{ar}^{\,2})(T + T_{ar})$ and another algorithm is used to incorporate the time step.

3.6 Specific heat as a function of temperature

As a body changes temperature the quantity of heat required to change the internal energy can be a

function of temperature. This quantity is commonly referred to as specific heat.

The variational form which includes only specific heat terms is:

$$I = \int_V (\alpha [N]\{T\}[N] \frac{d\{T\}}{d(t)} - [N]\{T\}Q)dV$$

If $\{\phi\} = [N]\{T\}$ then the $\frac{d\phi}{d\{T\}} = [N]^T$

defining $\alpha = \rho c$ where density is constant, then the variation of α with temperature can be expressed as two governing equations when using low carbon steel

$$\alpha_A = \alpha_1 + \alpha_2 (\frac{T_i + T_j + T_k}{3}) \text{ for } T < 775°K$$

and α_B = constant for $T \geq 775°K$

Again by taking the derivative and setting it equal to zero a minimum for this governing portion of the variational form is arrived at.

$$\frac{dI}{d\{T\}} = 0 = - \int_V [N]^T Q dV + \alpha_A \frac{d\left(\int_V [N]^T [N] dV \frac{d\{T\}}{dt}\right)}{d\{T\}}$$

$$+ \frac{d\alpha_A}{d\{T\}} \int_V [N]\{T\}[N] \frac{d\{T\}}{dt} dV$$

The derivative of α_A for temperatures less than 775°K is:

$$\frac{d\alpha_A}{dT} = \frac{\alpha_2}{3} \cdot \begin{Bmatrix} 1 \\ 1 \\ 1 \end{Bmatrix}$$

Going back to the minimized variation form the first term (including only Q) remains the same as derived earlier. The other two terms then become

$$\int_V \alpha_A [N]^T [N] dV \frac{d\{T\}}{dt} dV + \frac{\alpha_2}{3} \int_V [N]\{T\}[N] \frac{d\{T\}}{dt} dV$$

Using area coordinates for triangular elements and noting that:

$$[N] = [L_1, L_2, L_3]$$

the evaluation of the α_2 integral portion of the final two terms is

$$\frac{\alpha_2}{3} \int_A [L_1, L_2, L_3] \begin{Bmatrix} T_i \\ T_j \\ T_k \end{Bmatrix} [L_1, L_2, L_3] \, dA \quad \frac{d\{T\}}{dt} =$$

$$\frac{\alpha_2}{36} A \begin{Bmatrix} T_i \\ T_j \\ T_k \end{Bmatrix} \begin{bmatrix} 2 & 1 & 1 \\ 1 & 2 & 1 \\ 1 & 1 & 2 \end{bmatrix}$$

where $[L_1, L_2, L_3]\{T\}[L_1, L_2, L_3]$ equalled

$$[L_1^2 T_i + L_1 L_2 T_j + L_1 L_3 T_k,\ L_1 L_2 T_i + L_2^2 T_j + L_2 L_3 T_k,$$

$$L_1 L_2 T_i + L_2 L_3 T_j + L_3^2 T_k]$$

The α_A term was presented earlier and when combined with the α_2 term, specific heat adds only to the conductance matrix [C]

$$\left(\frac{\alpha_A A}{12} \begin{bmatrix} 2 & 1 & 1 \\ 1 & 2 & 1 \\ 1 & 1 & 2 \end{bmatrix} + \frac{\alpha_2 A}{36} \{T\}^T \begin{bmatrix} 2 & 1 & 1 \\ 1 & 2 & 1 \\ 1 & 1 & 2 \end{bmatrix} \right) \frac{d\{T\}}{dt}$$

and for $T < 775°K$

$$[C] = \left[\alpha_A + \alpha_2 \frac{\begin{Bmatrix} T_i \\ T_j \\ T_k \end{Bmatrix}^T}{3} \right] \begin{bmatrix} A \\ \overline{12} \end{bmatrix} \begin{bmatrix} 2 & 1 & 1 \\ 1 & 2 & 1 \\ 1 & 1 & 2 \end{bmatrix}$$

or for $T \geq 775°K$

$$[C] = \frac{\alpha_B A}{12} \begin{bmatrix} 2 & 1 & 1 \\ 1 & 2 & 1 \\ 1 & 1 & 2 \end{bmatrix}$$

Note that the additional term containing $\{T\}^T$ in the temperature range $< 775°K$ becomes unsymmetric.

3.7 Latent heats

Heat conduction in welding must include the change of phase. The dominant latent heat is that of fusion. The latent heat transformation has a value for steel of approximately 1/10 that of fusion and is considered minor in importance. Fusion usually occurs in temperature range for alloy steels from about 1700°K to 1755°K and therefore must be considered as a factor of heat input or withdrawal over that range.

During the welding process, as heat is input from the arc, there exists a liquid front surface, a solid front surface, and the in-between transition zone where latent heat is being absorbed (see Figure 5).

The opposite phenomenon takes place during the solidification process. Heat is given off in the transition zone as the metal is cooled which will increase the cooling time. The solid surface is represented by a 1700°K isotherm for steels while the liquid surface consists of the 1755°K isotherm. A method to incorporate latent heat was developed for the triangular element. The possibility of both the liquid and solid front intersecting a triangular element exists. This would create a complicated internal boundary problem to be solved for latent heat effects. By decreasing element sizes in this latent affected zone the number of elements affected by this internal boundary problem can be minimized. Then only a solid front or liquid front

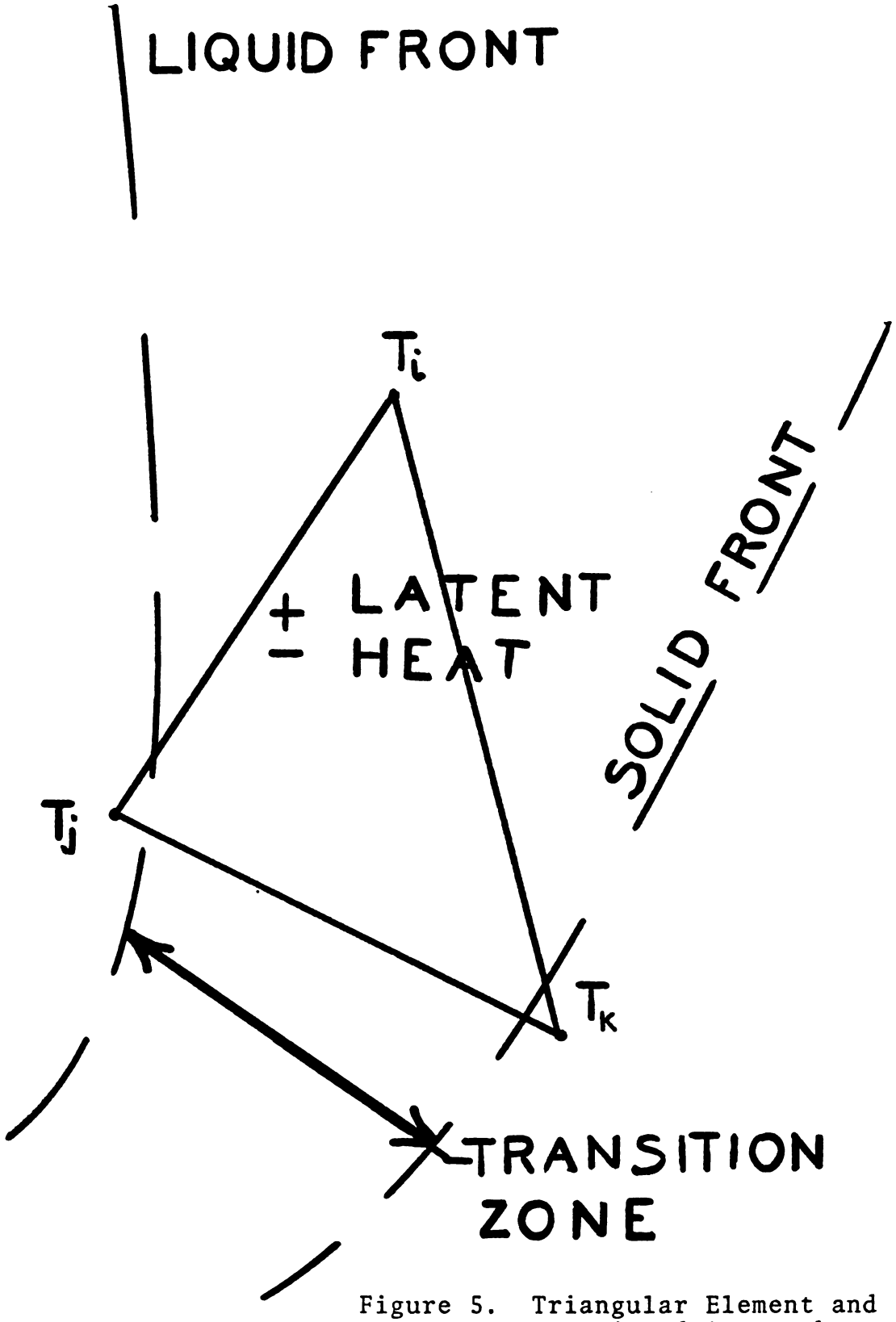

Figure 5. Triangular Element and associated latent heat surfaces.

would be intersecting a single element. This also creates a complex computational problem along with all the increased computer calculations used with temperature dependent properties. Therefore, a compromising assumption was made to approximate the true latent heat effects. The latent heat generated or given off within an element will be allotted equally to all three nodes of the triangle. To determine if an element is affected by latent heat an average temperature for the element is calculated:

$$T^e_{ave} = \frac{T_i + T_j + T_k}{3}$$

If T^e_{ave} falls within the latent heat range of 1700°K to 1755°K this particular element will then have a term added or subtracted to the force matrix. The sign of this term is either negative or positive corresponding to heat absorption and heat generation, respectively and the computer program was coded to a sign convention which is regulated by increasing or decreasing average element temperatures.

The portion of the functional affected is:

$$I = \int_V - (Q - \frac{\partial T}{\partial t}) \, T dV$$

Taking the derivative with respect to {T} yields:

$$\frac{dI}{d\{T\}} = -\int_V [N]^T Q \, dV$$

Since Q was assumed constant within the element this term becomes:

$$Q \int_V [N]^T dV$$

now $Q(\frac{\text{watts}}{\text{cm}^3})$ can be replaced by $\frac{\rho L}{\Delta t}$

where: ρ = density (for steel = 7.87 g/cm)

L = latent heat (for steel = 65.5 cal/gram)

Δt = length of a time step (seconds)

giving $\frac{\rho L}{\Delta t}$ units of $\frac{\text{watts}}{\text{cm}^3}$

The portion added to the force vector {f} is:

$$\frac{\rho L}{\Delta t} \int_V [N]^T dV$$

Which is:

$$\frac{\rho L V}{3\Delta t} \begin{Bmatrix} 1 \\ 1 \\ 1 \end{Bmatrix}$$

After the integral is evaluated.

Assuming a constant thickness this term is:

$$\frac{\rho LA}{3\Delta t}\begin{Bmatrix}1\\1\\1\end{Bmatrix}$$

Friedman (60) has a direct iteration method for phase change in finite element programs. He includes the ρL term as an addition to the ρc term and controls the implementation of the latent zone using a large number of coefficients.

3.8 Heat Flux Model

Friedman (55) states more reliable input data is needed in the finite element analysis to model the heat flux portion. This would yield a more thorough understanding of the welding process. He asks for more investigation of the physics of the welding arc. Andrews (48) and Muraki (28) express the intensity of the heat source, Q (Joule/m-sec) as:

$$Q = \frac{1}{h}\eta VI$$

where V = arc voltage (volts)

I = welding current (amperes)

η = arc efficiency

h = plate thickness (cm)

Again, the assumption of efficiency was made to the input data which because of the unsurety of its value can greatly vary results.

Friedman (55) assumed that heat of the welding arc to be a radially symmetric normal distribution function:

$$q(r) = q_0 e^{-Cr^2}$$

where q_0 and C are constants
determined by the magnitude and
distribution of the heat input
and r = distance from center of arc (m)

Westby (69) concurs with this distribution of specific heat flux, q (cal/sec cm^2), as being an approximation expressed by Gauss's distribution law. But, he simplifies it to a line or point source. He also gives efficiency factors for various welding processes which include heat losses due to radiation.

Verification of the heat flux distribution was done by Wilkinson (59). He used photographic techniques and pressure sensors to show this radial distribution (see Fig. 6). Assuming this radial distribution and setting the heat input equal to:

$$q_{total} = \int_0^\infty q(r) 2\pi r dr = \frac{q_0 \pi}{C} = Q$$

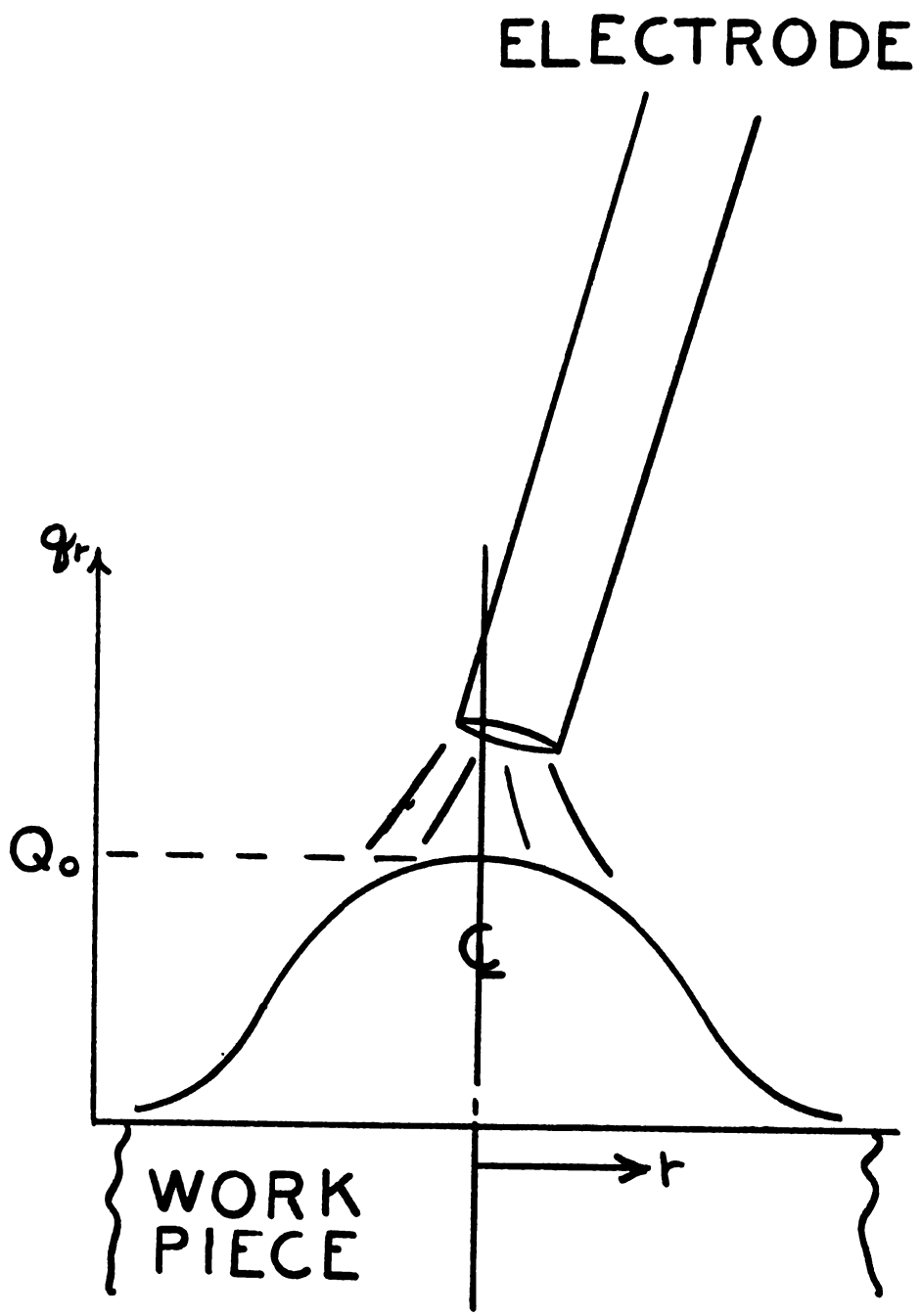

Figure 6. Heat Flux Distribution

where Q = Voltage x Amperage x Efficiency

The constant C can be solved for after assuming anything outside 5% of q_0 is negligible or for $q(\bar{r})$= 5% of maximum value (q_0)

$$q_{(r)} = q_0 e^{C\bar{r}^2} = .05\ q_0 \left(\frac{\text{watts}}{m^2}\right)$$

$$C = \frac{3.0}{\bar{r}}$$

But at present $\bar{r}$ can only be determined by photographic techniques. Only after $\bar{r}$ is determined or estimated can the distribution of heat flux be modeled.

Now r is the region in which 95% of the heat flux is transferred to the body.

Assuming a constant q ($\frac{\text{watts}}{m^2}$) across a triangular element boundary the portion added to the force matrix {F} is:

$$\frac{q\ L_{ij}}{2} \begin{Bmatrix} 1 \\ 1 \\ 0 \end{Bmatrix} \frac{\text{watts}}{m}$$

and heat flux was modeled as shown in Figure 7.
An improvement approaching exact values of q at element nodes can be achieved by using many small elements (see Figure 8). This approximation approaches a Guass distributed heat flux $q_i(r,t)$.

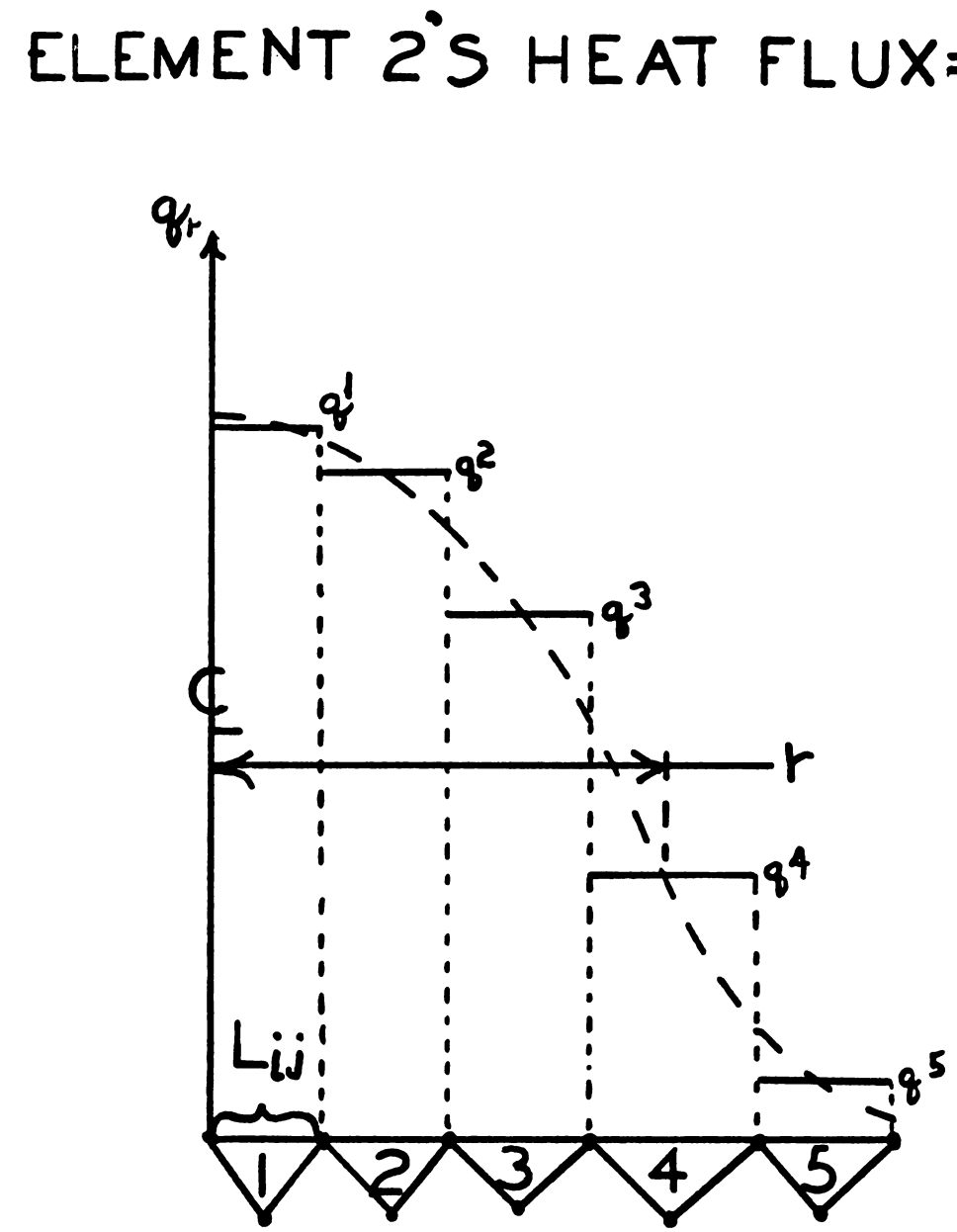

Figure 7. Model of constant q over an element side.

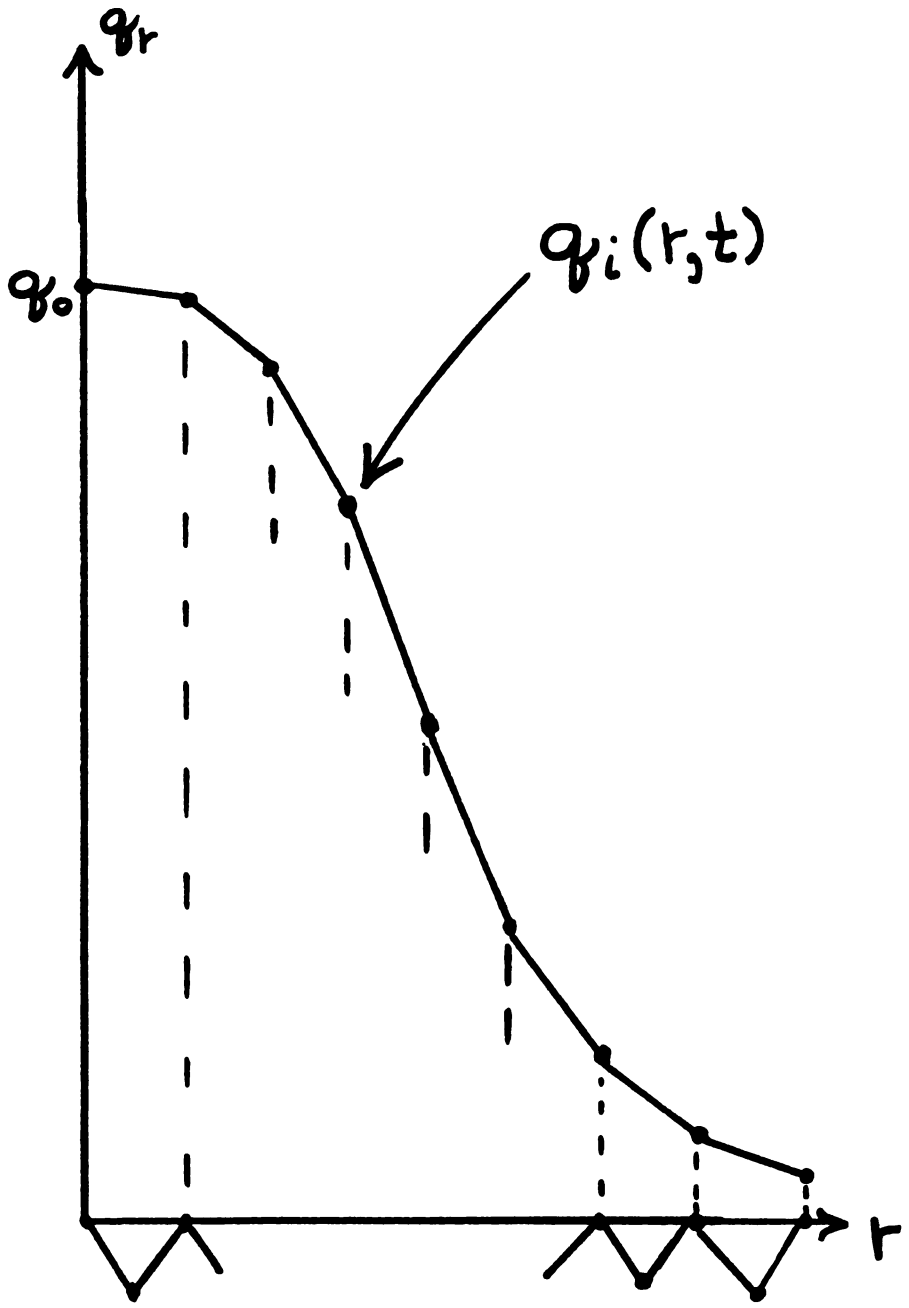

Figure 8. Heat Flux Model

q is given by:

$$q_i(r,t) = \frac{3Q}{\pi \bar{r}^2} \exp[-3(r/\bar{r})^2] \; EXP[-3(vt/\bar{r})^2]$$

where r = distance from center for a particular q_i (m)

v = velocity of the arc (m/second)

Q = total heat input (watts)

t = time (seconds)

q_i = watts/m at point i

$\bar{r}$ = maximum radius

At time equal to zero this equation has a heat flux distribution at its maximum for the two-dimensional plane being studied. Therefore, the above expression was backed up in time to model a passing arc by introducing a lag factor τ. The modified equation becomes:

$$q_i(r,t) = \frac{3Q}{\pi \bar{r}^2} EXP[-3r/\bar{r})^2] \; EXP[-3(\frac{V\{t-\tau\}}{\bar{r}})^2]$$

In this planar analysis it has been assumed the speed of the arc is high compared to the diffusion rate of the material so the amount of heat conducted ahead of the arc is relatively small to the total heat input. In order to make this a two-dimensional problem it has been assumed that the heat flow across the plane in the third dimension (direction of electrode travel) is again very small and negligible. Therefore, the $\frac{d}{dZ}[K\frac{\partial T}{\partial Z}]$

term goes to zero in the heat conduction equation.

3.9 Optimizing Weld Joint Strength

The design of a weldment has many variables affecting the outcome of how the joint can withstand various loading and environmental conditions. The design should consider that welding in some cases will result in significantly poorer properties than found in the base metal. The welded joint may be handicapped with lower fatigue strength caused by weld bead geometry, decreased toughness produced by microstructural changes in the heat affected zone or lowered corrosion resistance in certain environments caused by residual stresses. The control of stress concentration can be accomplished by varying the process, type of electrode, or doing post welding operations such as grinding. These are more of a state of the art fix to this problem. Residual stresses have no effect on lower carbon steel structures, so the problem of engineering a low carbon steel joint for maximum strength resolves to manipulation of the microstructure metallurgy in the heat affected zone. By controlling the high heat gradients over time the metallurgy of this area is controlled. Catastrophic failure of weldments by brittle fracture have been found in bridges, ships and other structures are usually caused by a reduced fracture toughness of the steel section. Again, the toughness of a weld joint is

affected by the high weld heat input over a short period of time. These heat gradients for any process are now determined by the thermo-finite element model previously developed.

Additional alloying elements added to steels help to increase strength such as grain size inhibitors of columbium or nitrogen. Deoxidation elements like aluminum or titanium secure fine grain sizes which aid in increasing steel toughness. Success in welding carbon steels is chiefly the ability to avoid the development of an unsuitable structure in or adjacent to the weld joint. Microstructural changes involving transformation of austenite, ferrite and martensite are the most important part and the cooling rate on the final structure being the most important parameter. Since heat input and metal mass of the joint have a wide range, the actual cooling rate may vary from fast rates to low rates. Other factors like joint design, electrode size, core wire composition, type of flux covering, kind of current and polarity of direct current have been found to have little influence on cooling rates.

Because of these fast cooling times in a welded joint, the iron-carbon diagram can no longer be used to determine the metallurgical structure. Continuous cooling transformation diagrams have been developed which more closely predict the microstructure of the

heat-affected zone. See Figure 9. Two researchers, Inagaki and Sekiguchi (10), studied the hardness and microstructure of the heat affected zone. They confirmed that the microstructure and hardness adjacent to the fusion line may be predicted from CCT diagrams. An example of how their prediction is approximated is shown in Figure 10. If the heat input during welding is small and cooling takes place at a rapid rate, the Z-cooling curve will depict the heat-affected-zone structure which will be entirely martensite and the hardness will be about 415 DPH. If the cooling rate should fall between the Z and F cooling curve some intermediate structure will result. Slower cooling of the structure resulting in values passing to the right of the F-cooling curves sees formation of some proeutectoid ferrite yielding a final structure of ferrite, an intermediate structure, and martensite. If cooling is carried out at a slower rate than the P-curve some pearlite structure develops. A further increase in cooling time beyond the E cooling curve enables the heat affected zone to be entirely ferrite and pearlite. Inagaki, et al. (10) found that the heat-affected zones which cooled at a sufficiently slow rate to produce some proeutectoid-ferrite did not crack spontaneously and exhibited a good degree of ductility and toughness. They concluded that this cooling rate which marked the appearance of proeutectoid ferrite be

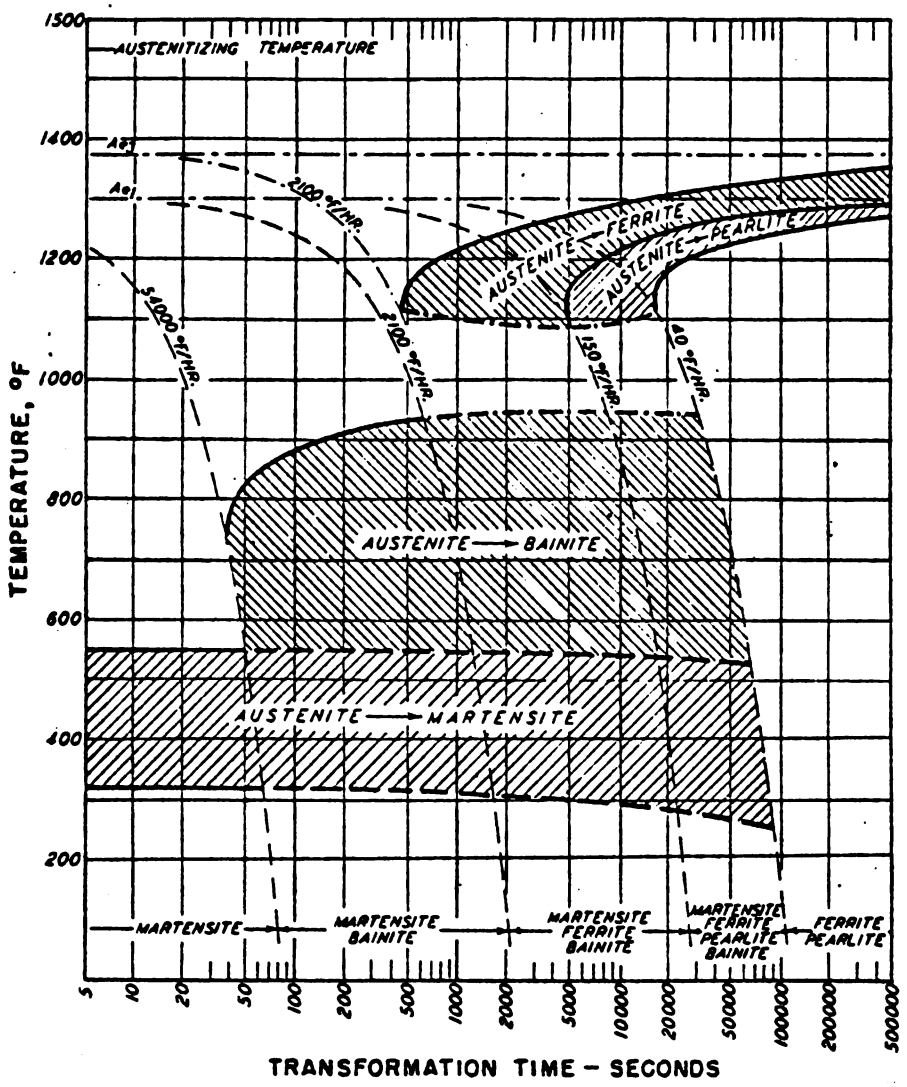

Figure 9. Example Continuous Cooling Transformation Diagram for Steel Ref (12) Page 1096.

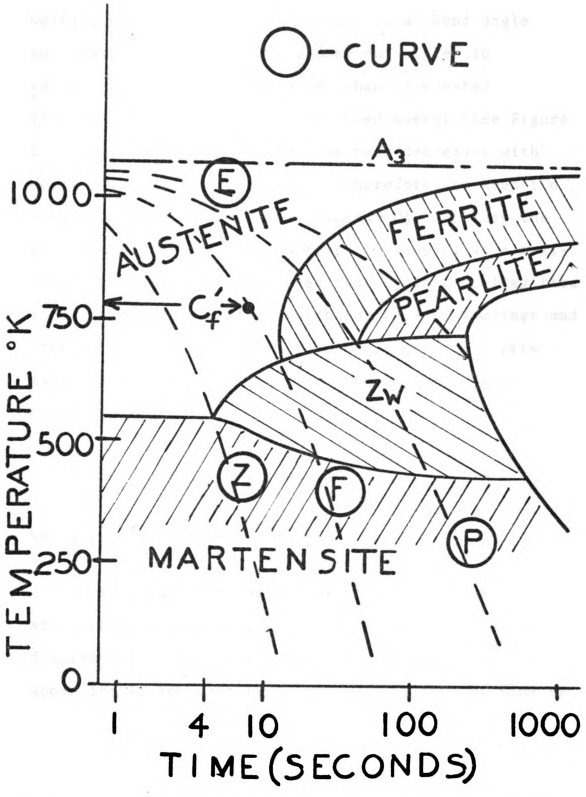

Figure 10. CCT Diagram showing critical pts, critical cooling curves, and critical cooling times.

marked by the symbol "C_f'" representing a limiting welding parameter. In their study total bend angle and Charpy Impact tests were done on samples to verify that cooling time longer than C_f' created larger bend angles and more absorbed energy (see Figure 11). These curves show that hardness decreases with cooling times greater than C_f'. Therefore, to keep the toughness at a maximum use a minimum C_f'. To keep the strength of the steel up, attempt to keep C_f' at a maximum. It then can be concluded that C_f' is a cooling time to optimize weld joint strength for various loadings and steels. From experimental results Inagaki (10) determined the minimum cooling time from the equivalent carbon content C_{eq}.

$$\log C_f' = 8.59\ C_{eq} - 1.69$$

$$\text{where } C_{eq} = \%\ C + \frac{1}{12}\ MN\% + \frac{1}{24}\ Si\%$$

It is known that the A_3 transformation point is affected by the metallurgy of the steel and the CCT diagram affected by how long the structure is heated above the A_3 temperature. To determine C_f', the time to cool between 1075°K to 775°K was considered to be the only general practical boundaries. The A_3 transformation temperature point is approximately 1075°K for mild and high tensile steels. For various other

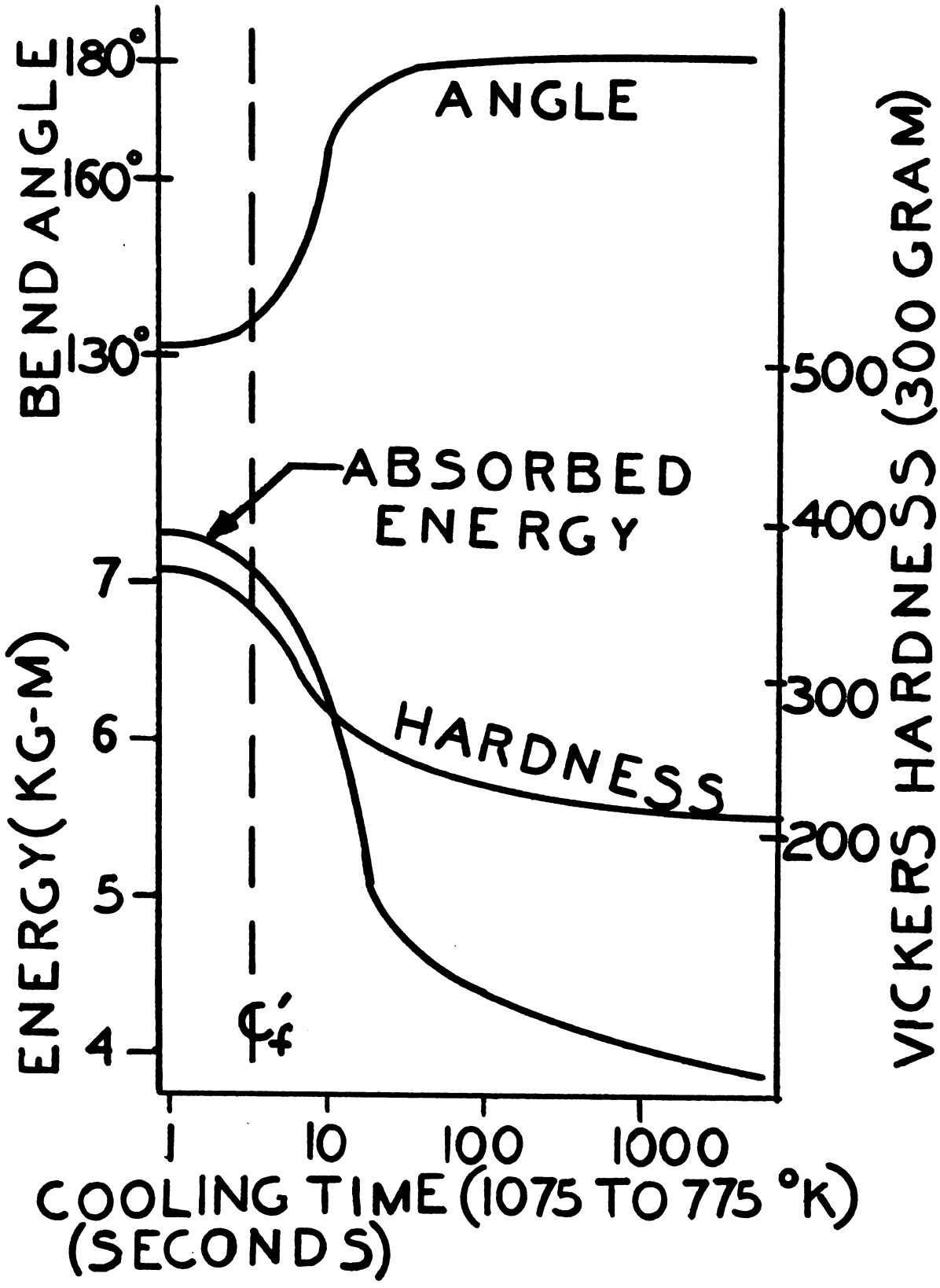

Figure 11. Cooling time versus hardness, bend angle and absorbed energy.

alloys the cooling time will have to be determined over a different range with 775°K still being the lower bound by definition of C_f'. Different welding processes didn't affect a typical hardness-cooling curve (see Figure 11). The hardness at C_f' has been found to be equivalent to Hv = 350 which is a maximum guideline set up by Welding Standards. At this hardness, no underbead cracks result in the heat affected zone and weld joint exhibits enough ductility.

A weld joint can be optimized by varying the input parameters to achieve the critical cooling time C_f' which will give maximum hardness at the fusion line without sacrificing bend tests angle. This can be calculated in a finite element program. For metallurgy determination away from the fusion line CCT diagrams will have to be referred to.

IV. Finite Element Program

4.1 Iterative Procedure

A Crank-Nicolson iterative method is used in solving the system of equations generated in this model. The implicit equation in matrix form is:

$$([K] + \frac{2}{\Delta T}[C])\{T_1\} = (\frac{2}{\Delta T}[C] - [K])\{T_0\} - 2(\frac{\{F_1\} + \{F_0\}}{2})$$

During each iteration the old temperature (prior iteration) $\{T_0\}$ is a known value along with values for [K], [C], and {F}. The solution gives the new temperatures $\{T_1\}$. Because some properties vary with temperature, [K] and [C] are reconstructed for each iteration. This process adds to computer execution time. A 539 element (303 nodes) model with a time step of .3 seconds required 13 minutes of computer execution time to simulate 75 seconds of real time.

The time step variable (ΔT) is important because its magnitude can affect the stability of the FEM solution. Fujii (72), Yalamanchili (71) and Chu (71) discuss stability in finite element schemes. Fujii re-

lates stability for the consistent mass case as restricted by the inequality:

$$\max\left(0,\ \alpha_0\ \left(\{1-2\theta\}\frac{\Delta T}{K_{min}^2}\right)\right) \leq \frac{2}{A_m(m+1)(m+2)}$$

A_m = 2 for simplex acute triangle

m = 2 for 2-dimensional case

K_{min} = minimum altitude of the triangle element

ΔT = time step

α_0 = $K/\rho c$

But when $\theta \geq 1/2$, the finite element scheme is unconditionally stable as is the case for this weld model because $\theta = 1/2$ (Crank-Nicolson).

4.2 Input Requirements and Output

The largest amount of input data consists of the element node numbers and their respective coordinates. To minimize punching over 500 cards (one for each element) and creating possible data errors an automatic grid generation program was used (62). This program included a node renumbering and optimizing subroutine which minimizes the bandwidth of the final system of equations (computer storage area needed for a matrix).

Besides element related information this weld program

requires the node numbers affected by radiation and heat flux. Their related element and coordinate values are subsequently supplied. The number of nodes, number of elements, and bandwidth are input and used to supply subroutines with variables regulating calculations and the building of [K], [C] and {F}.

Convection and radiation heat transfer are surfaces keyed off element grid data. Initial values for physical constants of thermal conductivity and specific heat are provided for these variables in subroutines. Other physical constants needed in calculations are ambient temperature, initial temperature, and the heat transfer convection coefficient. Iteration requirements include time step, number of iterations, and iterations between printed output. The arc velocity, maximum heat flux at the centerline, and 95% radius are the only variables needed to model the welding arc.

The output consists of the nodal temperatures at specific times after the beginning of welding. Also, during the arcing process heat flux is given at the element mid-point. Element number and appropriate surface of radiation or convection heat losses are printed for each iteration. All important physical quantities and element data are printed for convenience, as an analysis aid, and checking.

Figure 12 is a general flow diagram of this finite element weld model program. Figure 13 shows how the complete set of matrices are stored in the column {A} vector constructed in subroutine SETFL. Appropriate subroutines have been written to be compatible with manipulations of this A vector. A brief description of the subroutines is as follows.

SETFL - Sets the dimension of the column vector {A}

SETMAT - Constructs [C], [K] and {F} in {A}.

DCMPBD - Decomposes {A} into an upper triangle matrix.

TRANSNT - Heat flux calculated and output written

MULTBD - Combines right side terms of Crank-Nicolson equation

SLVBD - Solves for $\{T_{new}\}$ by backward substitution.

4.3 Thermal Conductivity and Specific Heat as Program Variables

It is difficult to choose the values of thermal conductivity, K, and specific heat, C, because they vary with temperature and material. As carbon content increases or alloying elements are changed the slope of the thermal conductivity versus temperature curve can change and even become positive (see Figure 2). The material was therefore restricted to low carbon steel (11).

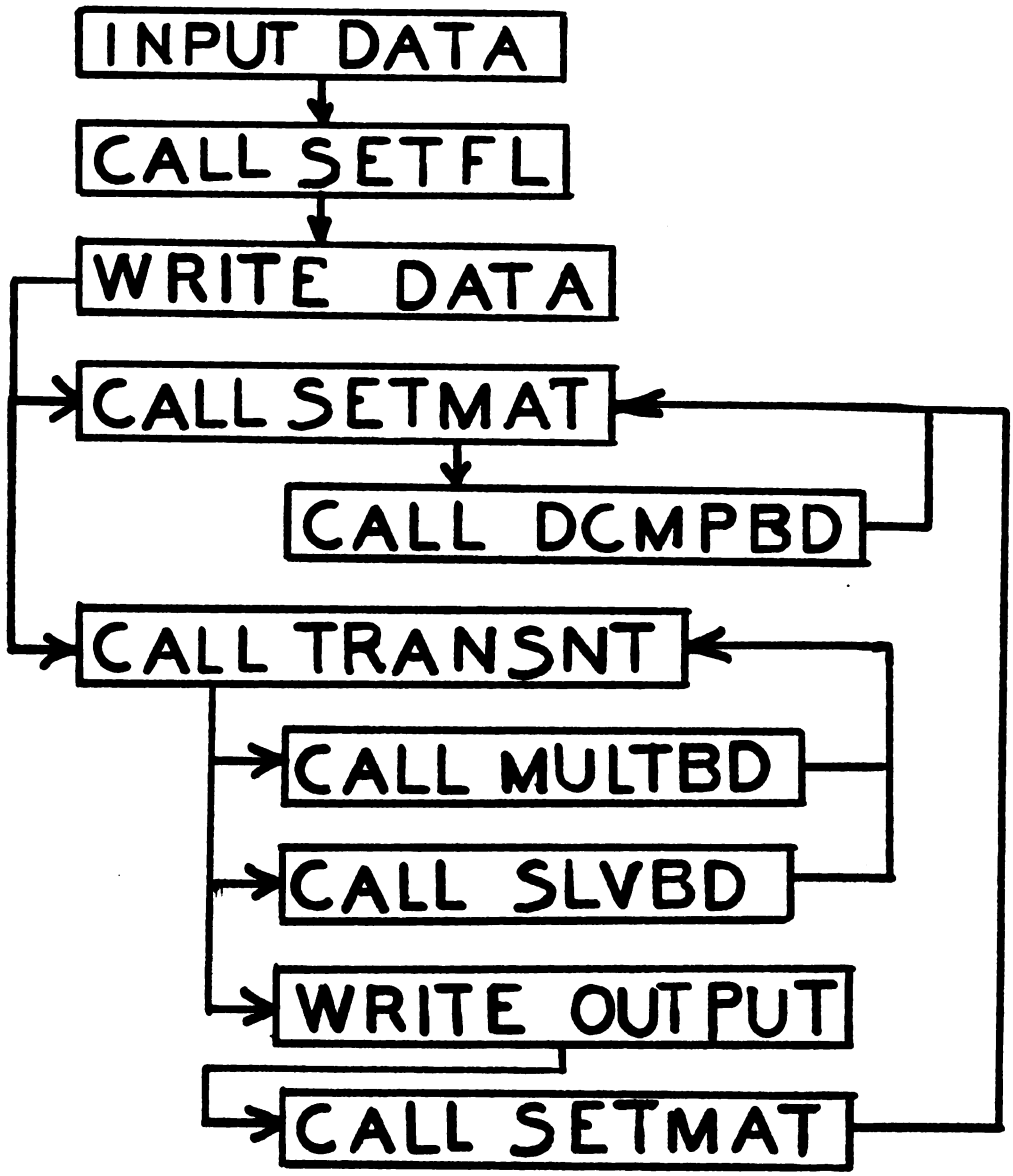

Figure 12. Computer Program Flow Diagram

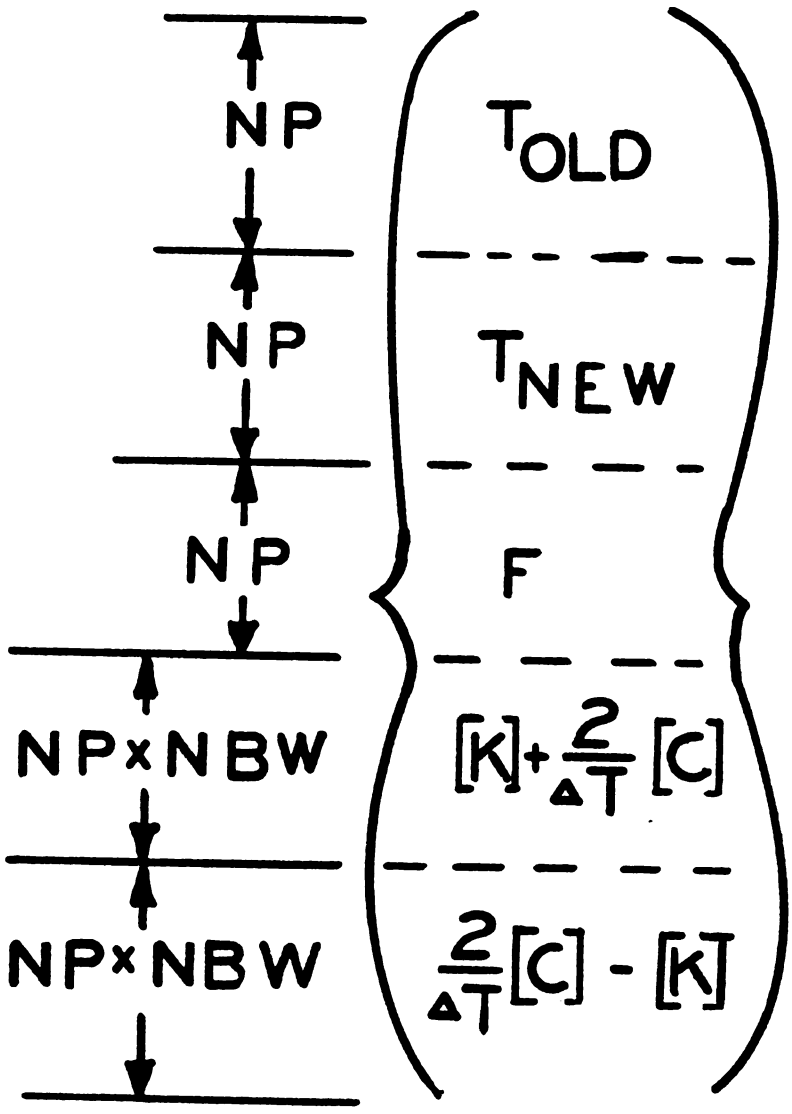

Figure 13. Storage in "A" Column Vector

Another variable, convection in the weld pool, changes the thermal conductivity from 1/5 of the value at room temperature to 3 or 4 times those values. Mizikar (73) has provided an estimate value of K in molten steel. Because of the need for further information U.S. Steel Corporation was contacted. Mr. Moore, U.S. Steel Corporation, (74) suggested using a value of approximately 2 times that of room temperature; a value commonly used in the industry.

The finite element model incorporated thermal conductivity as a function of temperature by using three relationships:

$$K_{xx} = .795 - .0004 * TAVE \text{ for } T < 1300\ ^\circ K$$

$$K_{xx} = .3\ \left(\frac{watts}{cm\ ^\circ K}\right) \text{ for } 1775\ ^\circ K > T \geq 1300\ ^\circ K$$

$$K_{xx} = .6 \text{ for } T \geq 1775\ ^\circ K$$

where TAVE = average of element nodal temperatures

$$= \frac{T_i + T_j + T_k}{3}$$

These equations would have to be changed when a different material is modeled or when welding under other convective patterns in the molten pool. A single constant value for thermal conductivity was calculated for each element.

Chapter 3 states thermal conductivity creates a

second term from the variational form when varied with temperature.

$$[K] = [K_C] + \underbrace{\frac{1}{6}[T_B]^T[K_B]}_{\text{second term}}$$

An estimate of the second term's influence on temperature results was performed. Analysis showed:

1. A minor (5%) importance when nodal temperatures vary by more than 300°K per element.
2. Decreased importance for small differences in nodal temperatures.
3. Further decreased importance for small elements.
4. Increased computer costs and execution time because of [K] becoming unsymmetric (4 times or more).

These results, especially the non-symmetry property, increase the cost of obtaining a solution and the additional second term was assumed negligible and not included in constructing [K]. The previous three K_{xx} equations then become part of $[K_C]$.

A similar second term results when specific heat is a function of temperature.

$$\frac{\alpha_A A}{12}\begin{bmatrix}2&1&1\\1&2&1\\1&1&2\end{bmatrix} + \underbrace{\frac{\alpha_2 A}{36}\begin{bmatrix}2&1&1\\1&2&1\\1&1&2\end{bmatrix}}_{\text{second term}}$$

Again, because of non-symmetry and a similar importance analysis yielding negligibility for the second term, this term was not included in constructing [C]. Specific heat was modeled as:

$\rho c = 1.3 + .0053 * TAVE$ for $T < 775°K$

$\rho c = 5.0$ for $T \geq 775°K$

ρ = density assumed constant

The average of nodal temperatures determines specific heat which was assumed constant over an element.

4.4 Additions to the Force Vector

Heat flux is added to the force vector by a distribution presented in Chapter 3 for $q_i(r,t)$. Heat flux was calculated for a radius equaling the midpoint of an element and divided equally between the pair of nodes and added to the force matrix. Using the heat flux model in Chapter 3, τ was determined by

$\tau = \bar{r}/V$

$\bar{r}$ = radius including 95% of q

V = arc velocity

This heat flux model provided a gauss distribution approaching Figure 8 as the size of the elements gets very small in the arc area.

When heat flux isn't an input to the force vector either convection or radiation from the surface is dominant. For steels 675°K is an approximate break-even point between these two surface related properties.

Latent heat was added to the force matrix during the solidification process if the average temperature of the element was between 1700-1755°K (common for alloy steels). The derivation of this addition is given in Chapter Three. If melting occurred, latent heat was subtracted from the force vector. The program limited the occurrence of an addition or subtraction of latent heat to a one time phenomenon.

The reinforcement of a weld pool (filler added) was not modeled by additional elements, but temperatures of melted nodes were allowed to go to 4000°K providing accountability for this phenomenon. Other modeling where reinforcement wasn't present the maximum allowable nodal temperature was 3500°K. This is an important limitation because the elements are finite in size and radiation influence does cause instability with higher than 4000°K surface temperatures.

V. Verification and Sensitivity Analysis

5.1 Verification with Christensen's and Hess' Work

In order to be confident that the finite element model is approximating an actual weld, a comparison with actual thermocouple experiments was made. Two groups of researchers, Hess (19) and Christensen (49), have done extensive recording of time-temperature relationships for a range of welding applications. Their data was used to verify the accuracy of this numerical model. Three comparisons which show close agreement between experimental and finite element approximation are given in Figures 14, 16, 17.

Figure 14 is a comparison of thermocouple readings and the finite element model (Figure 15) in the HAZ. After a considerable time-lapse (50 seconds from arc passing) the two begin to differ by as much as 10% with the experimental readings being lower. This could very well be the effect of the thermocouple's drilled hole creating a heat loss boundary lowering local temperatures. The key area of the curve, critical cooling time, correlates well and the values of C_f' are almost equal. This alone shows that this finite element

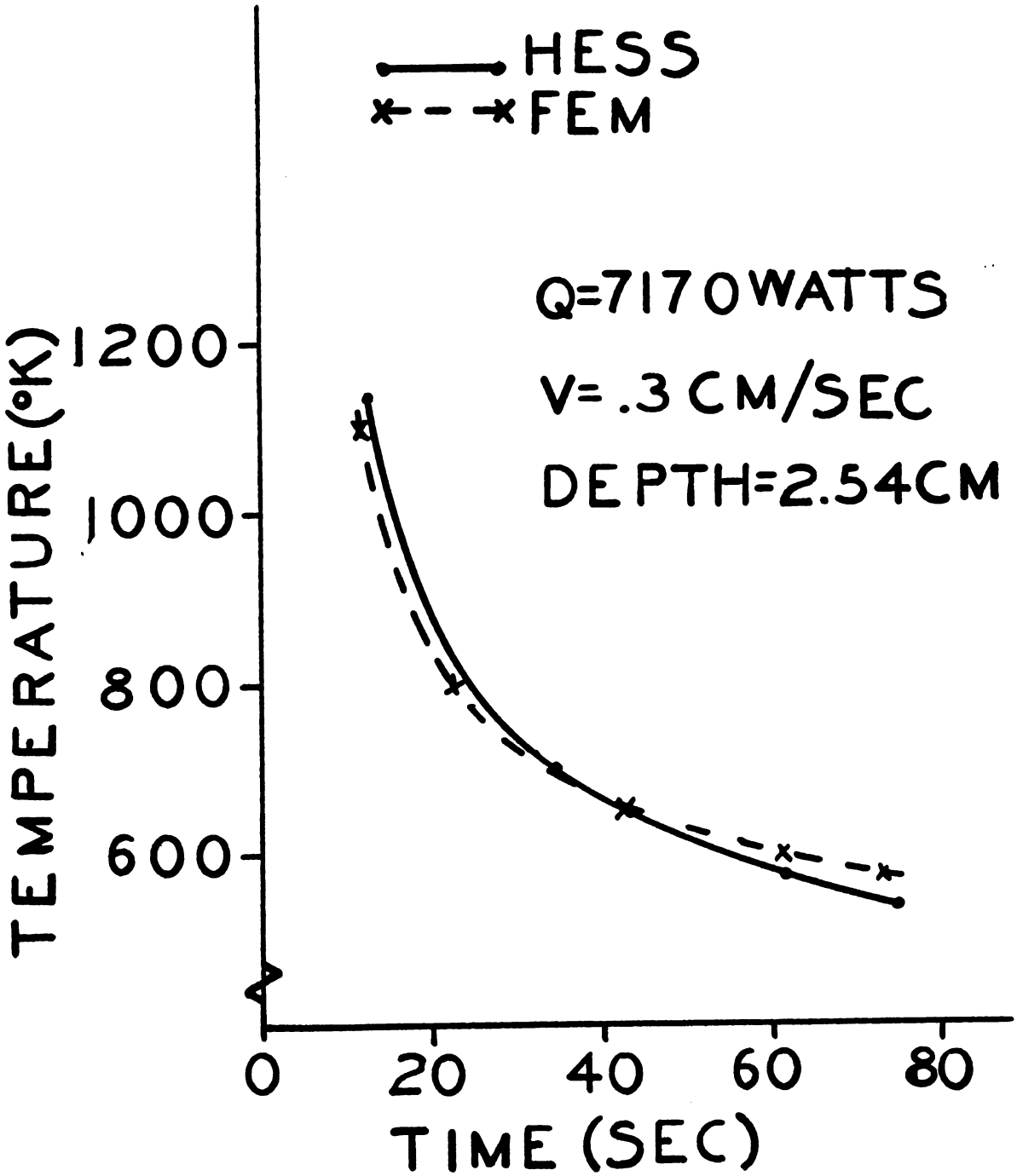

Figure 14. Verification with Hess's work (time-temperature curve)

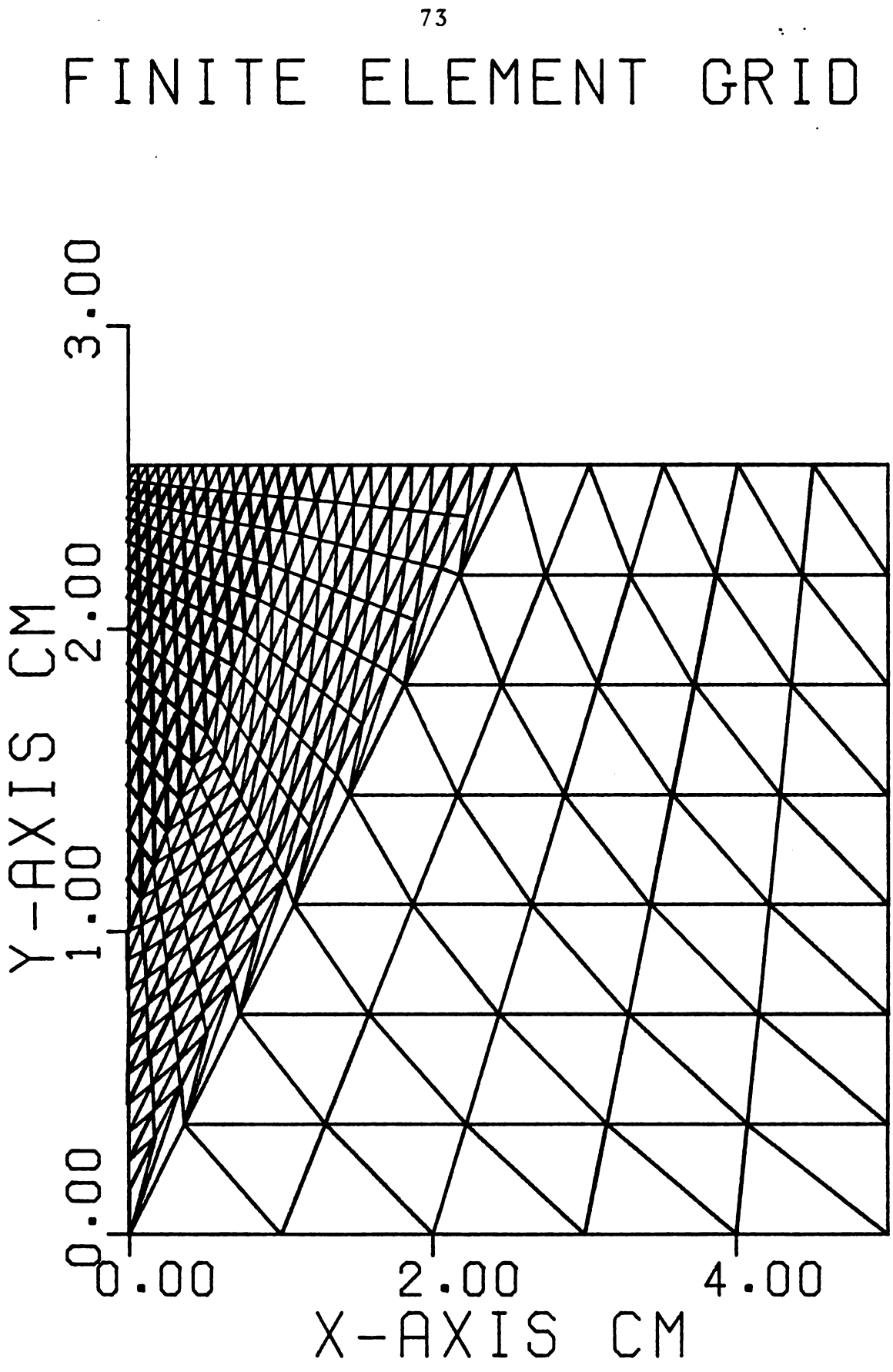

Figure 15. Element Model of Hess' Work

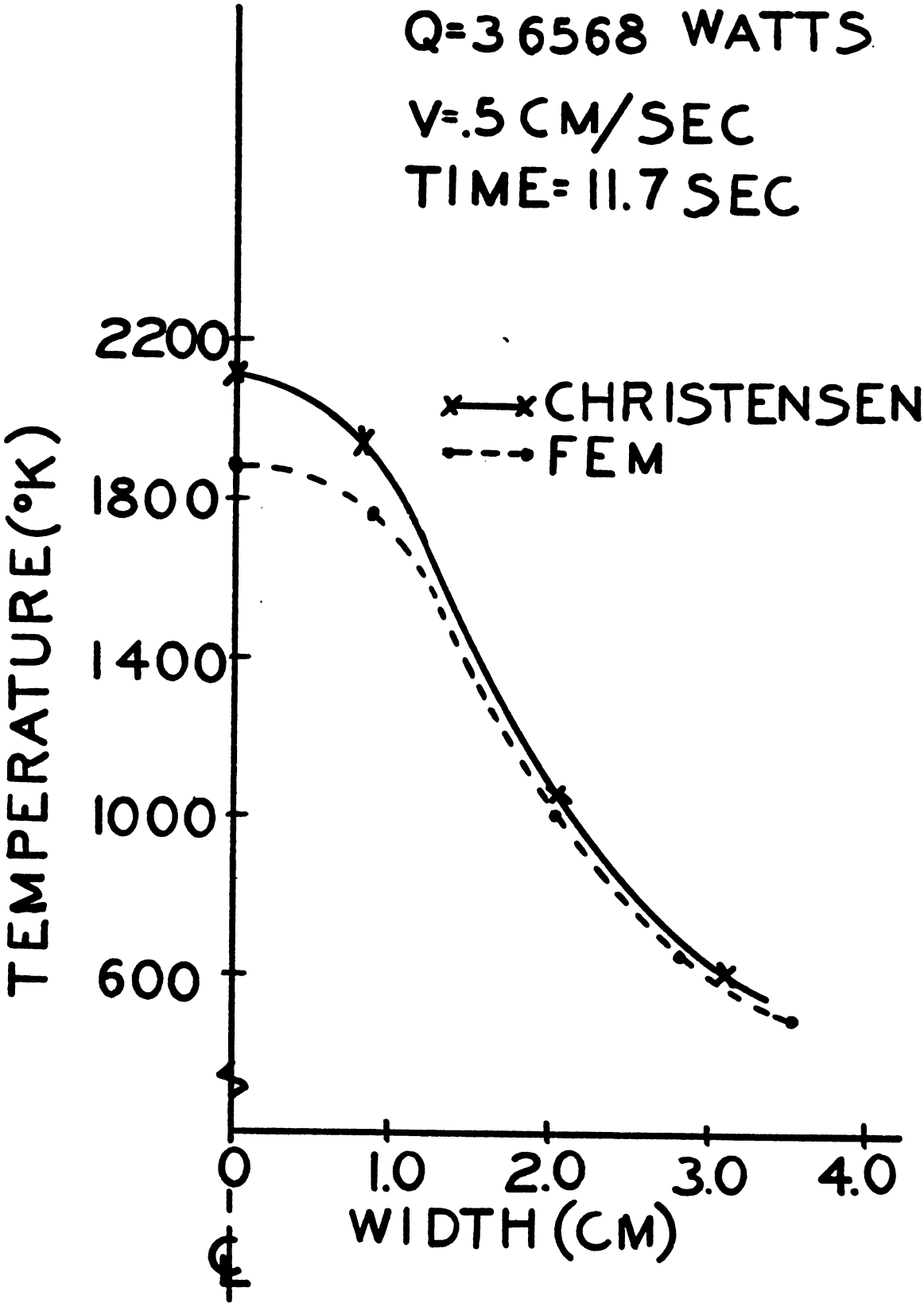

Figure 16. Cross Section Temperature Verification

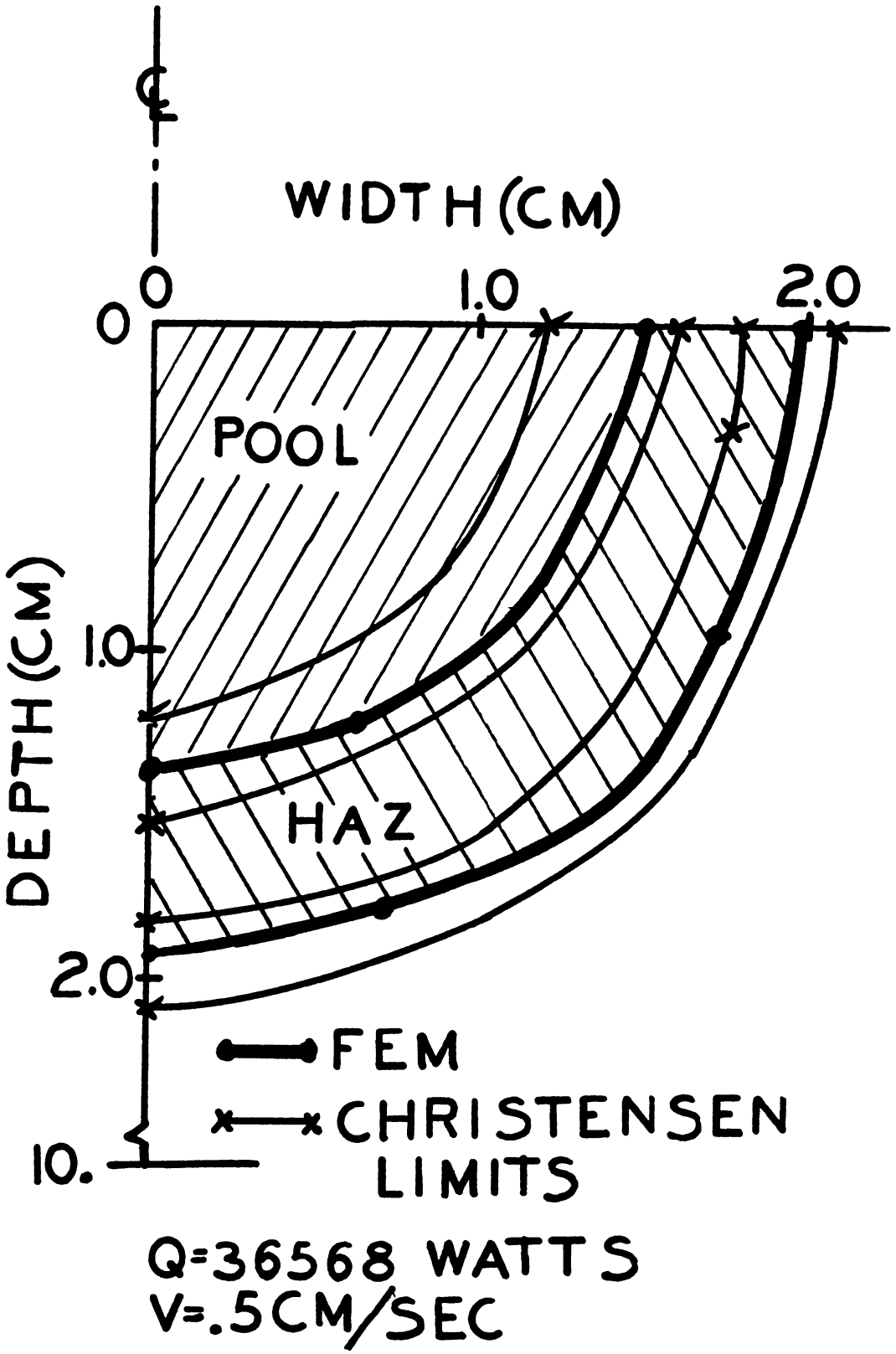

Figure 17. Verifying Model Weld Pool and HAZ Sizes

model gives a close approximation to actual welding conditions.

Figure 15 relates Christensen's work with the modeling of a submerged-arc process. The FEM model is in close agreement with experimental data in the heat affected zone (1.5-2.0 cm) which is the most important correlation area. Only in the weld pool does the finite element result vary by more than 5% from experimental. In this area of variation thermal conductivity of molten steel being erratic might provide reasoning for the difference. But, Christensen stated that his thermocouple measurements were very inaccurate in the pool. Values ranged from 2500°K to 3500°K and depended how measurements were taken.

Adding another dimension to this finite element model's versatility approximate solidus line and HAZ can be determined. This is depicted in Figure 17. Again, Christensen's data had scatter in it relating the difficulty in measuring this process. The FEM approximation of the heat affected zone and weld pool correlate well with experimental results falling within Christensen's established bounds.

5.2 Sensitivity of Some Variables

5.2.1 Radius of the Welding Arc

The area affected by the heat flux is regulated by the 95% containment radius $\bar{r}$. This radius is currently

determined by photographic estimation.

A sensitivity analysis was done on the influence of $\bar{r}$ on the finite element solution because of the unsurety of its value. This analysis was done by varying $\bar{r}$ from .5 cm to 1.5 cm using Christensen's welding parameters. A node in the heat affected zone was chosen to determine the effects of various welding arc radii. Figure 18 shows a plot of time-temperature values and how they are affected by varying $\bar{r}$. From this graph it can be depicted that $\bar{r}$ affects the size of the weld pool, size of the heat affected zone and critical cooling time. Therefore, the welding arc must be accurately modeled for meaningful results to be obtained from numerical methods.

Since little research has been done in arc modeling and its shape highly influences finite element results, more work is needed. Possible use of inverse conduction methods might provide accurate arc dimensions and heat transfer efficiencies of welding processes.

5.2.2 Thermal Conductivity in the Weld Pool

A heat affected node was used as the basic location for estimating the sensitivity of the FEM solution to variations in weld pool thermal conductivity. Three different values of thermal conductivity were used and the effect on temperature relationships are shown in

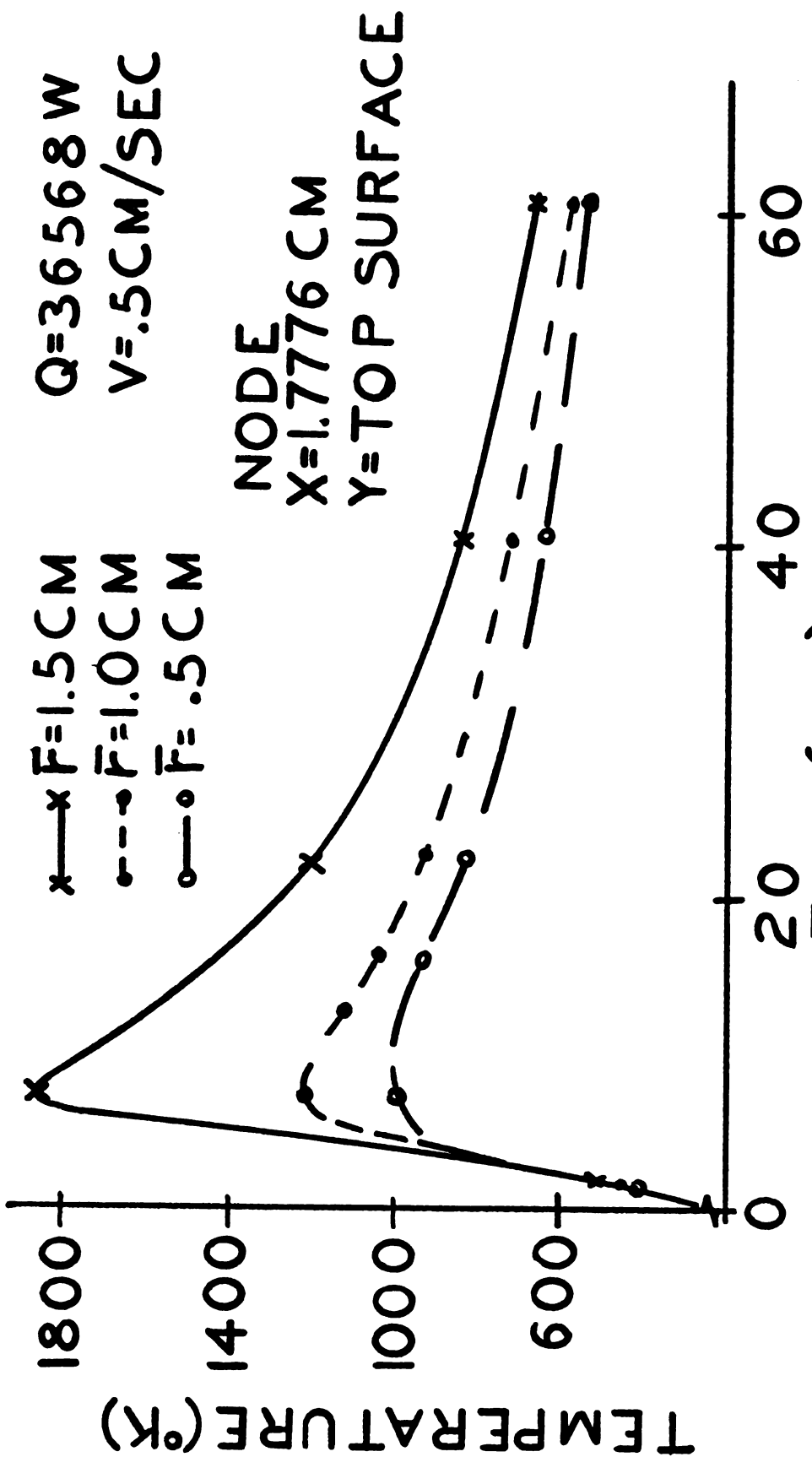

Figure 18. Sensitivity to Welding Arc Radius

Figure 19. As K varied from .2 watts/cm°K to a value of 1.2 watts/cm°K, the temperature history experienced by the surface location varied from one extreme of not even getting hot enough to enter the HAZ to reaching melting temperatures.

The relationship of higher thermal conductivity values creating higher maximum temperatures makes FEM solutions very sensitive to this variable.

5.2.3 Convection Coefficient and Emissivity Value

Boundary conditions can vary and their effect on the finite element model was checked. Figures 20 and 21 are plots of various common values for the heat transfer coefficient (free convection) and the emissivity of steel in the molten area (T > 1700°K). Variations in each of these variables changed the solution by minor amounts. The heat transfer coefficient produced only a 6°K difference while the emissivity is a little greater with a difference in nodal temperatures up to 19°K in the HAZ. The solution results are considered insensitive to these variables.

5.2.4 Grid Coarseness and Time Step

The element grid used to compare Christensen's work is shown in Figure 22. This grid model has a fine mesh in the area of high thermal gradients. A comparison

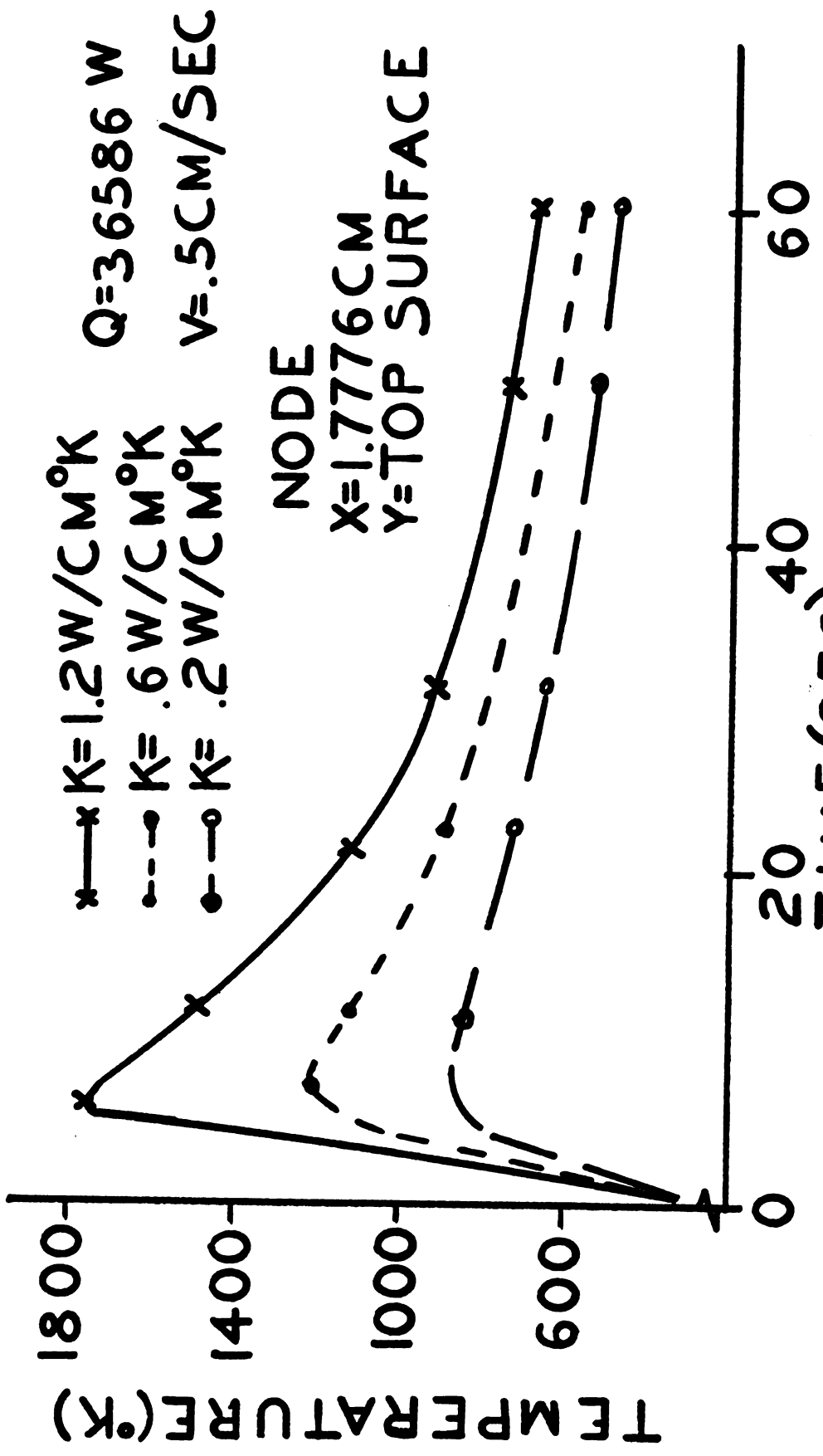

Figure 19. Sensitivity to Weld Pool Thermal Conductivity

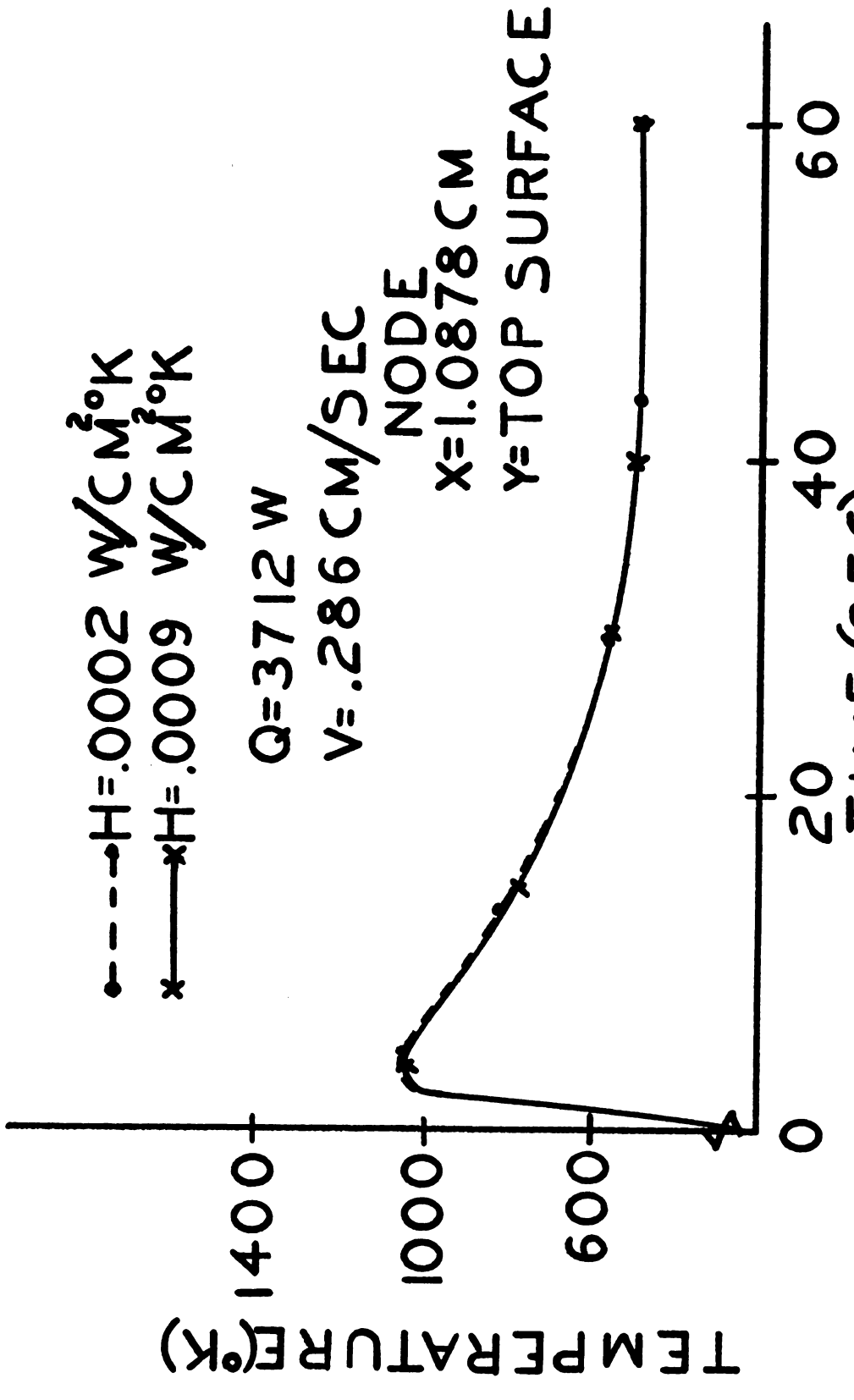

Figure 20. Sensitivity of Convection Coefficient

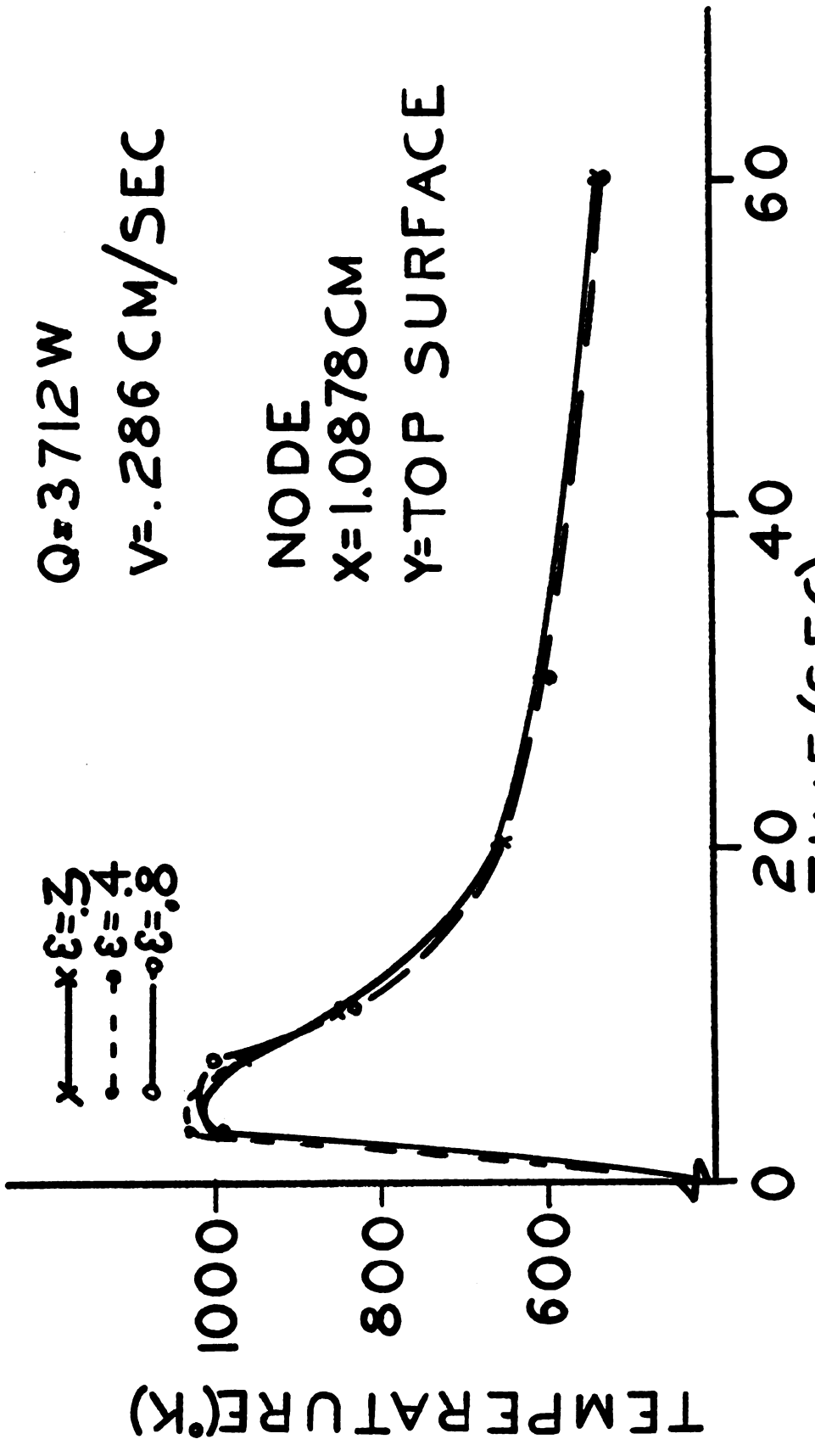

Figure 21. Sensitivity of (ε) Emissivity in Molten Area

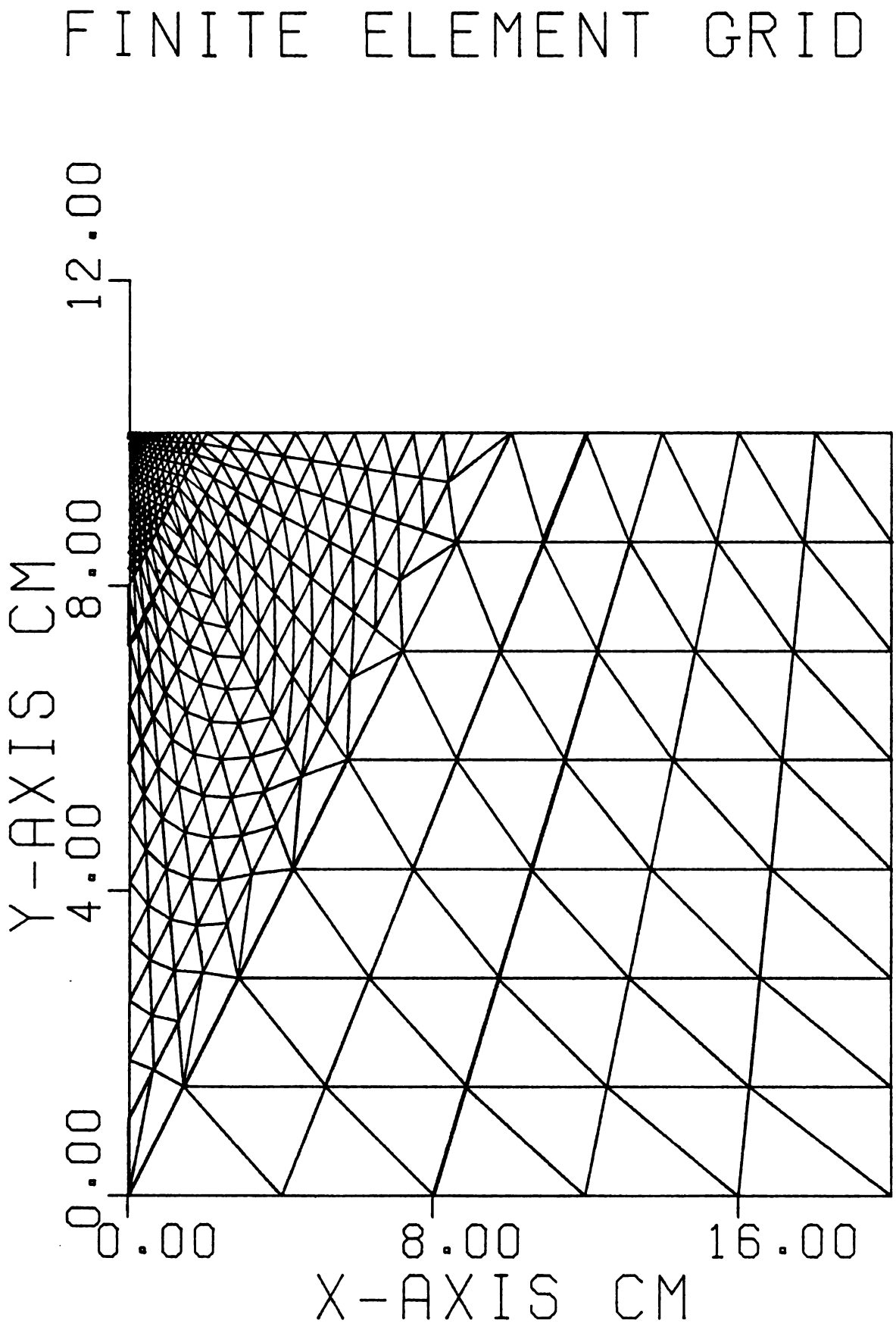

Figure 22. Fine Grid Model

of results with a coarser grid (Figure 4) is graphed in Figure 23. The coarser grid does not adequately transmit heat in the weld area and results in a lower temperature curve.

The choice of grid size is an engineering judgment when using finite element approximations. It plays an important part in getting accurate results with small elements a must criteria for high gradient areas.

Figure 24 depicts the sensitivity of two different time steps on the finite element solution. ΔT of .3 and .1 seconds were compared. Little variation resulted in the HAZ temperatures, but some instability at high temperatures (1800°K on up) was seen when the smaller time step was used. Increasing the time step to determine its effects was ruled out by the need to plot results using small steps.

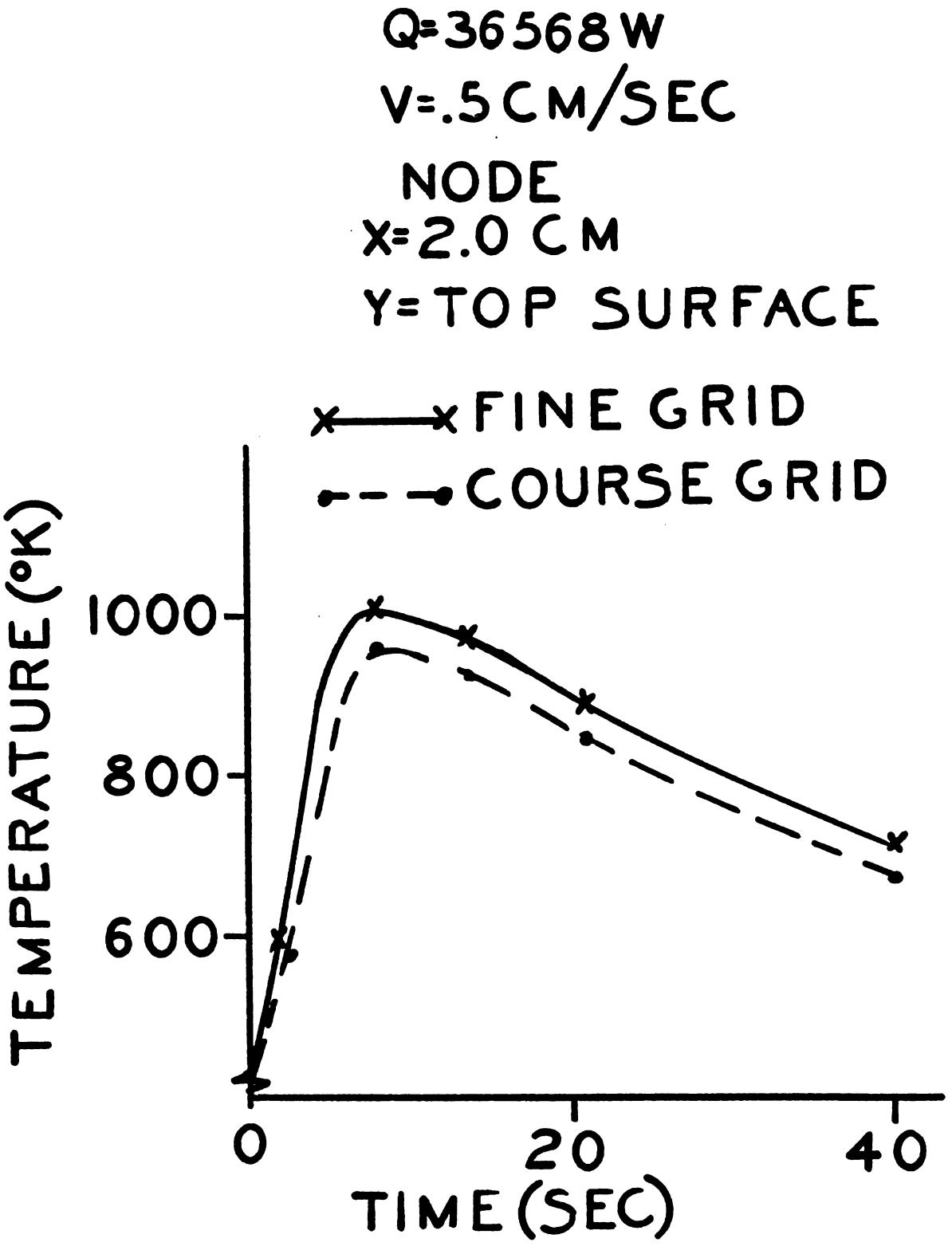

Figure 23. Coarse Versus Fine Grid

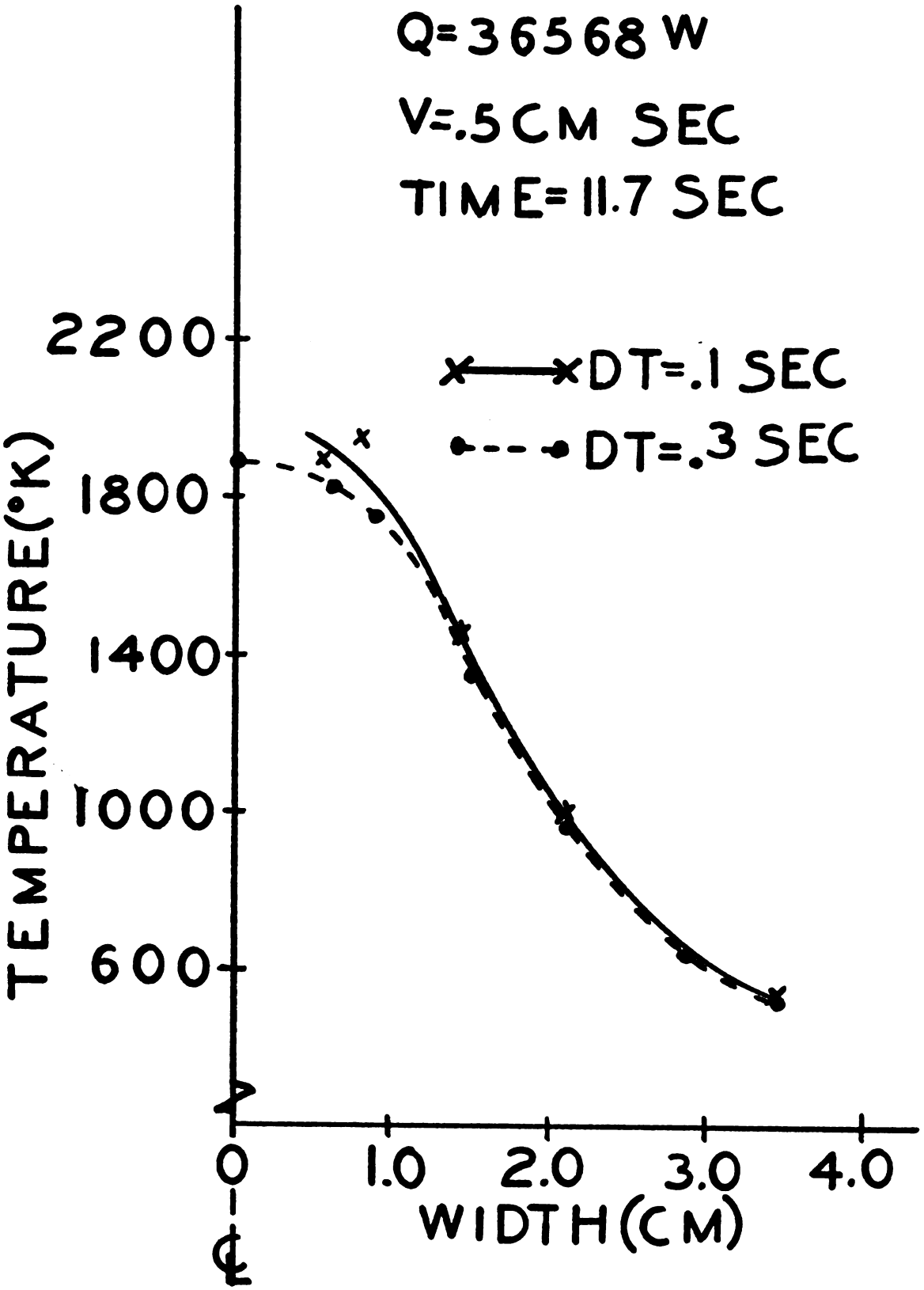

Figure 24. Comparison of Two Time Steps

VI. Application to Welding Design

6.1 Joint Strength

The total joined area regulates the strength in the static loading of welded joints. This area can be determined from the finite element model. The only variable needed in static load calculations not determined by the FEM model is the weld reinforcement stress concentration which is a state of the art function primarily related to the type of welding rod, the angle of the arc, and the arc velocity.

For dynamic loading cases, such as fatigue, the toughness of a joint regulates its strength over time. Inagaki's (10) report lays the ground work for maximizing the energy absorbed by a joint (toughness) with his critical cooling time factor. This C_f' is the optimum cooling time to obtain maximum strength at maximum toughness. C_f' is estimated by Inagaki's experimental equation:

$$\log C_f' = 8.59\ C_{eq} - 1.69$$

The finite element model results were used to calculate the cooling time for a proposed set of welding parameters.

If the cooling time varies from Inagaki's optimum, the welding parameters can be varied to optimize the joint strength by meeting the C_f' criteria. Some parameters that affect C_f' are arc velocity, size of the electrode, type of welding process, backup plates, physical size of the base metal, and material constituents. The advantage of using the finite element model in optimizing C_f' is the ease of changing variables and the ability to obtain results of the temperature history in a matter of minutes.

6.2 Effect of Arc Velocity on Cooling Time

To depict how one of the aforementioned variables can be changed to optimize C_f', the arc velocity effect was looked at. Critical cooling time is defined as the time to cool the HAZ from 1075° K to 775°K. The examples of C_f' location in Figure 25 are in agreement with Inagaki's critical location (the fusion line). As a HAZ node (or location) approaches the fusion line the cooling rate becomes faster and more critical. Little difference in C_f' is seen between internal and surface nodes on the fusion line.

An example of arc velocities' effect of C_f' is shown in Figure 26. The velocity was varied from .2 to 1.5 cm/sec causing the temperature history of one HAZ surface node to change considerably.

To show the effect of different velocities on C_f'

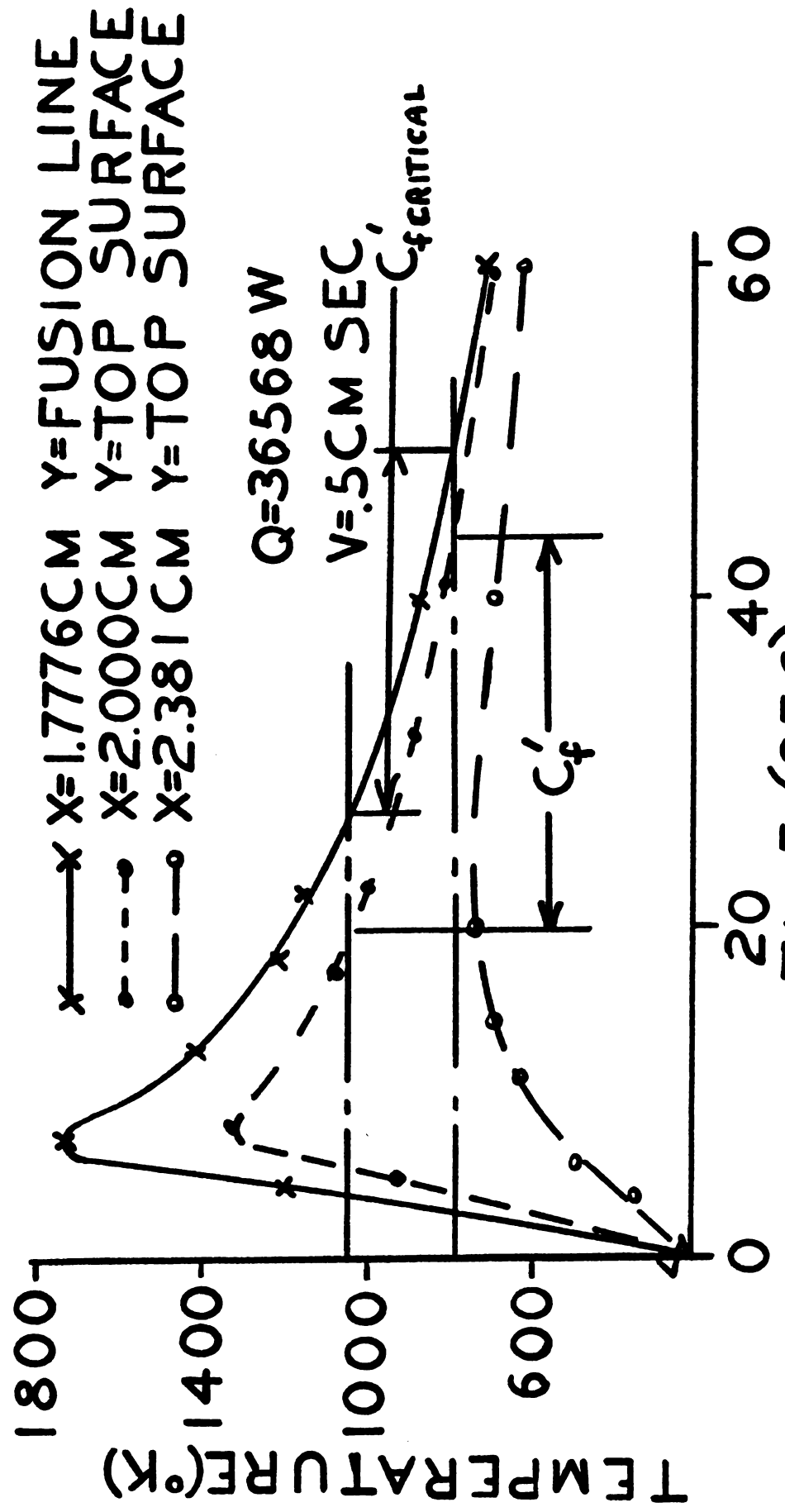

Figure 25. Minimum Cooling Time Determination

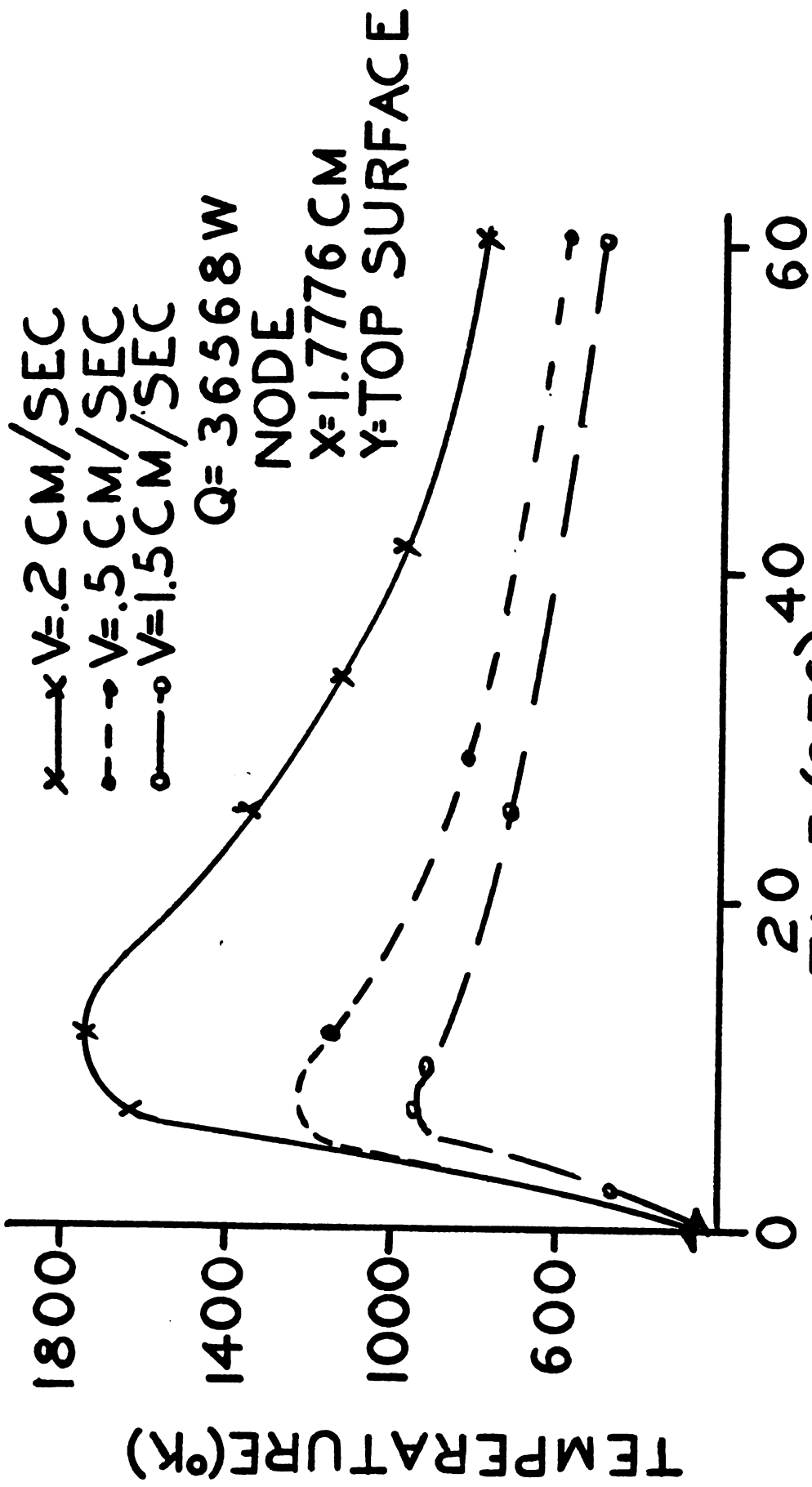

Figure 26. Arc Velocity Effects on a Node Cooling

temperature histories for fusion line nodes were plotted in Figure 27. It can be concluded from these plots that increasing C_f' can be accomplished by slowing the speed of travel. The speed of travel also interacts with melt depth, where slower speeds result in larger depths.

Before the use of these conclusions become a recommendation, economic factors must be considered. Items such as welding time costs may lead to a compromise in final joint conditions.

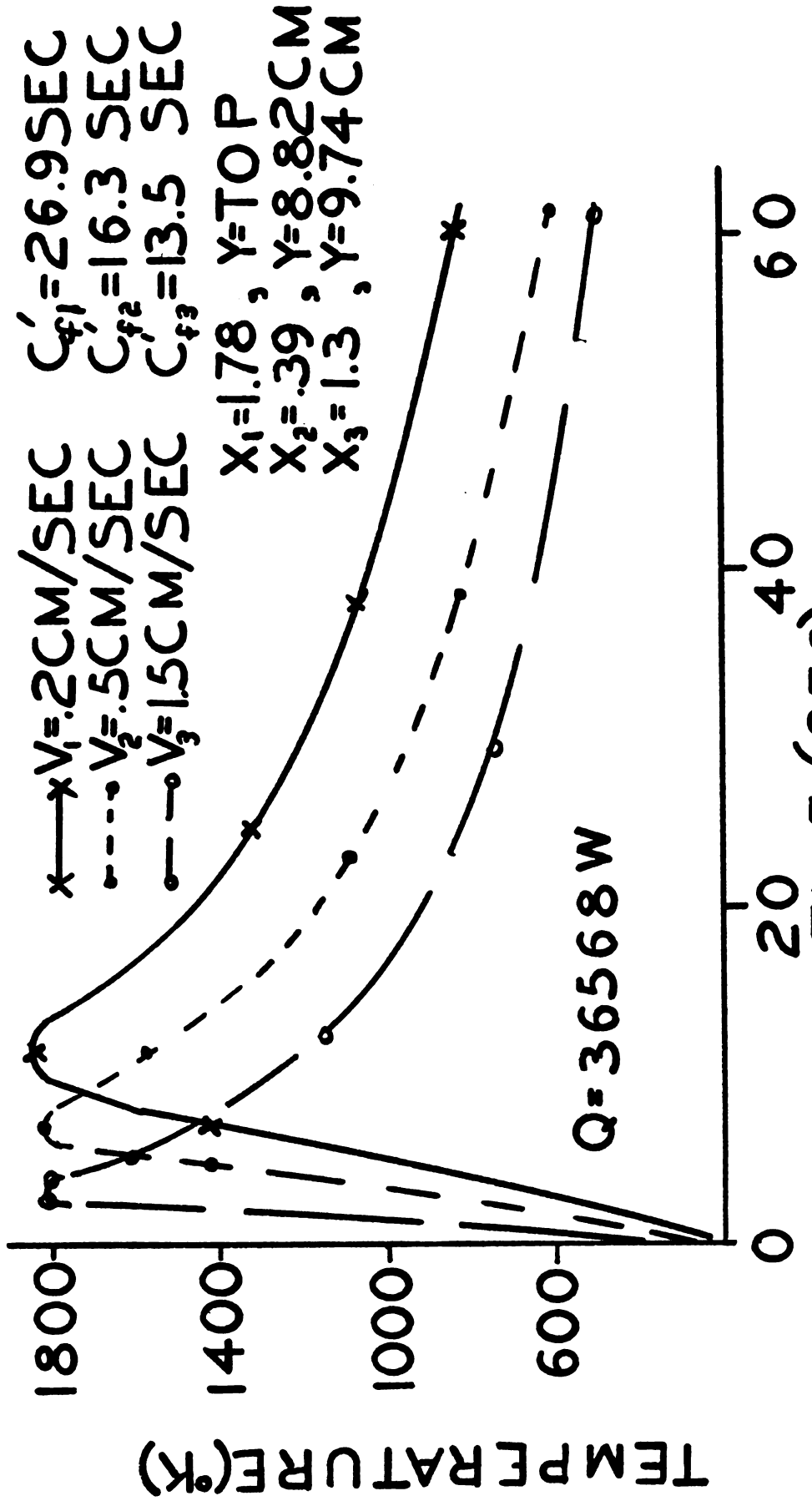

Figure 27. Effect of Velocity on C'_f

VII. Summary and Conclusions

The finite element method was used to obtain the time-temperature relationship in a butt welded joint. This transient thermal history influences the metallurgical properties in the heat affected zone. By varying certain welding parameters, the weld joint strength can be optimized when a certain metallurgical structure is achieved.

The finite element computer program used simplex triangular elements, included specific heat and thermal conductivity as functions of temperature, incorporated latent heat of fusion, and convection and radiation heat losses from the surface.

The following conclusions were drawn from this study:

1. The non-linear finite element method model closely approximates actual welding conditions but must be used cautiously because the results are sensitive to the arc radius and the thermal conductivity of molten steel.
2. The fusion line-top surface intersection is an acceptable location to use in estimating critical cooling time.

3. Slowing the arc velocity increases the cooling time of the fusion line.
4. Heat affected zone and penetration can be determined with this method. If joint strength is insufficient in weld depth, the correct value can be arrived at by varying heat input or arc velocity.

VIII. Recommendations for Further Study

This study is the beginning of the application of the finite element numerical technique in the area of welding and casting. Only the surface of a large volume of possible research paths has been scratched. Results presented should help those continuing onward in this area. By pursuing some of the recommendations, future researchers assist in solving a vast number of practical and theoretical engineering problems.

1. Basic physical property research is needed on thermal conductivity in weld pool temperature ranges.
2. Weld arc distributions should be determined for all processes. This might be done numerically using an inverse heat conduction approach (65).
3. Material could be saved in the casting industry if a three-dimensional finite element model could be developed.
4. Expand this model to include slag and weld reinforcement. The use of higher order elements may improve results and reduce computer costs. Their use should be investigated.

5. Fatigue test various joints to assure the critical cooling time is an optimizing parameter.
6. Incorporate the non-symmetric temperature dependent terms of thermal conductivity and specific heat into [K] and [C] and determine if the results have been improved in the high heat gradient areas.
7. Develop mathematical bounds for time steps of various finite elements to assure stability of the solution.
8. Model other weld configurations such as spot, fillet, and pre-notched joints.
9. Develop a FEM model for the welding of other materials including aluminum, plastics and high strength steel.
10. Apply these thermal history results to the elastic-plastic FEM models.

REFERENCES

REFERENCES

(1) Rosenthal, D. "Mathematical Theory of Heat Distribution During Welding and Cutting." The Welding Journal, pp. 220S-234S. May 1941.

(2) Rosenthal, D. "The Theory of Moving Sources of Heat and Its Application to Metal Treatments." Transactions of ASME, pp. 849-866. Nov. 1946.

(3) Rosenthal, D. and R. Schmerber. "Thermal Study of Arc Welding. Experimental Verification of Theoretical Formulas." The Welding Journal (17) pp. 2-8. April 1938.

(4) Mahla, E. M., M. C. Rowland, C. A. Shook, G. E. Doan. "Heat flow in Arc Welding." The Welding Journal, pp. 459S-468S. Oct. 1941.

(5) Dolby, R. E. and G. G. Sanders. "Metallurgical Factors Controlling the Heat Affect Zone Fracture Toughness of Carbon: Manganese and Low Alloy Steels." Welding Institute Report II WDoc. IX-891-74.

(6) Lancaster, J. F. Metallurgy of Welding, Brazing, and Soldering. G. Allen & Unwin, London, p. 45-69. 1965.

(7) Stout, R. D. and W. D. Doty. Weldability of Steels. Welding Research Council, New York, NY. p. 831. 1953.

(8) Henry, O. H. Welding Metallurgy. American Welding Society, New York, NY. 3rd Edition. 1965.

(9) Linnert, G. E. Welding Metallurgy. Vol. 2, American Welding Society, New York, NY. 3rd Edition. pp. 309-395. 1957.

(10) Inagaki, M. and H. Sekiguchi. "Continuous Cooling Transformation Diagrams of Steels for Welding and their Applications." Transactions of the National Research Institute for Metals (Japan) Vol. 2, N 2. pp. 102-125, 1960.

(11) Goldsmith, A., I. E. Watermour and A. J. Hisschhorn. Handbook of Thermophysical Properties of Solid Materials, Vol. II, Pergamon Press, 1963.

(12) McGannon, H. The Making, Shaping and Treating of Steel, 9th Edition 1971. Printed by Herbick and Held Pittsburgh, Pennsylvania for US Steel Corporation.

(13) Republic Alloy Steels. Republic Steel Corp., Cleveland, OH 44101. 1968.

(14) Materials Properties Handbook. Hartford House, London. Vol. II, 1966.

(15) 1975 SAE Handbook. Society of Automotive Engineers, Warrendale, PA. Vol. 1.

(16) Adams, Clyde M. "Cooling Rate and Peak Temperatures in Fusion Welding." The Welding Journal, pp. 210S-215S, May 1958.

(17) Paley, Zui, J. N. Lynch and C. M. Adams. "Heat Flow in Welding Heavy Steel Plate." The Welding Journal, pp. 715-795, Feb. 1964.

(18) Paley, Z. and P. D. Hibbert. "Computations of Temperatures in Actual Weld Designs," Report Pm-m-74-2. Dept. of Energy, Mines and Resources, Ottawa, Canada, March 12, 1974.

(19) Hess, W. F., L. L. Merrill, E. F. Wippes, and A. P. Bunk. "The Measurement of Cooling Rates Associated with Arc Welding, and Their Application to the Selection of Optimum Welding Conditions." The Welding Journal, pp. 377S-422S, Sept. 1943.

(20) Paschkis, V. "Establishment of Cooling Curves of Welds by Means of Electrical Analogy," IBID, pp. 462S-438S, Sept. 1943.

(21) Iwamura, Y. and E. F. Rybicki. "A Transient Elastic-Plastic Thermal Stress Analysis of Flame Forming." Journal of Engineering for Industry, pp. 163-171, Feb. 1973.

(22) Rybicki, E. F. and L. A. Schmit, Jr. "An Incremental Complementary Energy Method of Non-Linear Stress Analysis," AIAA Journal Vol. 8 No. 10, pp. 1805-1812, Oct. 1970.

(23) Ghadiali, N. D. and E. F. Rybicki. "An Analytical Technique for Evaluating Deformation Due to Welding." Battelle Lab Report, Columbus, Ohio. Aug. 1974.

(24) Dawes, M. G. "Residual Stresses and Strains in Weldments." The Welding Institute Research Bulletin, pp. 264-268, Sept. 1974.

(25) Schofield, K. G. "Residual Stress Measurement Techniques." IBID, pp. 74-79, March 1975.

(26) Faupel, J. Engineering Design. John Wiley and Sons, New York, NY, pp. 658-909, 1964.

(27) Lubkin, J. L. "Structural Modeling of a Welded Joint Typical for Vehicle Frames." Michigan State University, Div. of Engr. Research, Dec. 31, 1973.

(28) Muraki, T., J. J. Bryan, and K. Masubuchi. "Analysis of Thermal Stresses and Metal Movement During Welding. Part I - Analytical Study." Transactions of ASME. Journal of Engineering Materials and Technology, 74-WA/MAT-4, pp. 1-4, 1974.

(29) Muraki, T., J. J. Bryan and K. Masubuchi. "Analysis of Thermal Stresses and Metal Movement during Welding. Part II Comparison of Experimental Data and Analytical Results." IBID, pp. 1-7, 1974.

(30) Whiteman, J. R. A Bibliography for Finite Elements. Academic Press, London, 1975.

(31) Wilson, E. L. and R. E. Nickel. "Application of the Finite Element to the Heat Conduction Equation." Nuclear Engineering and Designs 3. pp. 1-11, 1966.

(32) Aguirre-Ramirfz G. and J. T. Oden. "Finite Element Technique Applied to Heat Conduction in Solids with Temperature Dependent Thermal Conductivity." ASME Paper 69-WA/HT-34 N.P. 13, 1969.

(33) Donea, J. and S. Giuliani. "Code Tafest Numerical Solution to Transient Heat Conduction Problems using Finite Elements in Space and Time." Report ER-5049, Joint Nuclear Research Centre, European Atomic Energy Commission, ISPRA, Italy, 1974.

(34) Visser, W. "A Finite Element Method for the Determination of Non-Stationary Temperature Distribution and Thermal Deformations." Proc. 1st Conf. Matrix Methods in Structural Mechanics, Wright Patterson AFB, OH10, A FFDL Tr 66-80, 1965.

(35) Visser, W. "The Finite Element Method in Deformation and Heat Conduction Problems." DELFT. 1968.

(36) Wilson, E. L., K. J. Bathe and F. E. Peterson. "Finite Element Analysis of Linear and Non Linear Heat Transfer." Paper L1/4, Proceedings and Structural Mechanics in Reactor Tech. Conf. Berlin, 1973.

(37) Hutula, D. N., B. E. Wiancko and S. M. Zeiler. "Apache a Three-Dimensional Finite Element Program for Steady State or Transient Heat Conduction Analysis. Report WAPD-IM-1080, Bettis Atomic Power Laboratory, Pittsburgh, 1973.

(38) Jfzernik, A. and A. Leech. "The Comparison of Iterative and Direct Solution Techniques in the Analysis of Time-Dependent Stress Problems, Including Creep, by the Finite Element Method." pp. 449-462 of J. R. Whiteman (F.D.) The Mathematics of Finite Elements and Applications. Academic Press, London, 1973.

(39) Segerlind, L. J., R. P. Singh, J. G. P. De Baerdemaeker and R. J. Gustafson. "Theoretical Aspects of the Finite Element Method." ASAE Paper 74-5501 pp. 1-28, Dec. 1974.

(40) Segerlind, L. J., R. P. Singh, J. G. P. De Baerdemaeker and R. J. Gustafson. "Computer Implementation of the Finite Element Method." IBID. Paper 74-5502, pp. 1-10, Dec. 1974.

(41) Segerlind, L. J., R. P. Singh, J. G. P. De Baerdemaeker and R. J. Gustafson. "Element Data Generator for Some Two-Dimensional Finite Element Programs." IBID 74-5503 pp. 1-19, Dec. 1974.

(42) Segerlind, L. J., R. P. Singh, J. G. P. De Baerdemaeker, and R. J. Gustafson. "Some Finite Element Programs for Agricultural Engineering Instruction." IBID. No. 74-5504 pp. 1-39, Dec. 1974.

(43) Bruch, J. C. and G. Zyvoloski. "Transient Two-Dimensional Heat Conduction Problems Solved by the Finite Element Method." Int. J. Numer. Meth. Eng. 8, pp. 481-494, 1974.

(44) Comini, G., S. D. Guidice, R. W. Lewis and O. C. Zienkiewicz. "Finite Element Solution of Non-Linear Heat Conduction Problems with Special Reference to Phase Change." Int. J. Numer. Meth. Eng. 8, pp. 613-624, 1974.

(45) Fujino, T. and K. Chsaka. "Heat Conduction and Thermal Stress Analysis by the Finite Element Method." Proc. 2nd Conf. Matrix Methods in in Structural Mechanics, Wright-Patterson AFB., Ohio AFFDL-TR-68-150, 1968.

(46) Fullard, K. "The Computation of Temperature Distributions and Thermal Stresses using Finite Element Techniques." Paper M5/3 Proc. 1st Structural Mech. in Reactor Tech. Conf. Berlin 1971.

(47) Naehrig, T. H. and J. P. Gaschen. "The Calculation of Three-Dimensional Temp. Dist. and Thermal Stresses using Finite Element Method." Paper M5/2, IBID.

(48) Andrews, J. B., M. Arita, and K. Masubuchi. "Analysis of Thermal Stress and Metal Movement During Welding." NTIS Report N71-26143., Dec. 1970.

(49) Christensen, N., V. de L. Davies, and K. Gjermunsden. "Distribution of Temperatures in Arc Welding." British Welding Journal, Vol 12, pp. 54-75, Feb. 1965.

(50) Roberts, Doris K., A. A. Wells. "Fusion Welding of Aluminum Alloys." Part V. IBID. Vol. 1 pp. 553-560. 1954.

(51) Zienkiewicz, O. C. The Finite Element Method in Engineering Science. McGraw-Hill, London, 1971.

(52) Singh, R. P. and L. J. Segerlind. "The Finite Element Method in Food Engineering." ASAE Paper No. 74-6015. pp. 1-18, June 1974.

(53) Meyers, P. S., Uyehara, O. A., and Borman, G. L. "Fundamentals of Heat Flow in Welding," Welding Research Council Bulletin, No. 123, July 1967, pp. 1-46.

(54) Finite Element Application to Vehicle Design, International Conference on Vehicle Structural Mechanics SAE Conference Proceedings Detroit, Michigan. March 26-28, 1974. pp. 1-285.

(55) Friedman, E. "Thermomechanical Analysis of the Welding Process Using the Finite Element Method." Transactions of ASME. Paper 75-PVP-27, 1975, pp. 1-8.

(56) Hibbitt, H. D., and Marcal, V. P. "A Numerical Thermo-Mechanical Model for the Welding and Subsequent Loading of a Fabricated Structure," Computers and Structures, Vol. 3, pp. 1145-1174, Perganon Press 1973.

(57) Westby, Ola, Element Methods for Welding Deformations and Residual Stresses, Special Lecture, 1975, Technical University of Norway.

(58) Kohler, W. and Pittr, J. "Calculations of Transient Temperature Fields with Finite Elements in Space and Time Dimensions," International Journal for Numerical Methods in Engineering, Vol. , 1974, pp. 625-631.

(59) Milner, D. R. and Wilkinson, J. B. "Heat Transfer From Arcs," British Welding Journal, February 1960, pp. 115-128.

(60) Friedman, E. "A Direct Iteration Method for the Incorporation of Phase Change in Finite Element Heat Conduction in Programs," Report WAPD-TM-1133, U.S. Atomic Energy Commission, March 1974.

(61) Toyooka, T., and Watanabe, M. Embrittlement in Weld Stain-Affected Zone in Carbon Steel, Special Report - Kawasaki Heavy Industry, LTD. Kobe, Japan.

(62) Segerlind, L. J., Applied Finite Element Analysis, John Wiley and Sons, New York, NY 1976.

(63) Strang, G. and Fix, G. An Analysis of the Finite Element Method. Prentice-Hall Inc., 1973.

(64) Beck, J. V. "Nonlinear Estimation Applied to the Nonlinear Inverse Heat Conduction Problem," International Journal of Heat and Mass Transfer, Vol. 13, pp. 703-716. Pergamon Press, 1970.

(65) Beck, J. V. "Criteria for Comparison of Methods of Solution of the Inverse Heat Conduction Problem," ASME Paper 75-WA/HT-82. pp. 1-11, 1975.

(66) Beck, J. V. "Determination of Optimum Transient Experiments for Thermal Contact Conductance," International Journal of Heat and Mass Transfer, Vol. 12. pp. 621-633. Perganon Press 1969.

(67) Report on Physical Properties of Metals and Alloys from Cargogenic to Elevated Temperatures, ASTM, Publication Number 296, 1960. pp. 51-58.

(68) Report on Elevated-Temperature Properties of Wrought Medium-Carbon Alloy Steels, ASTM, Publication No. 199, 1957.

(69) Westby, Ola "Temperature Distribution in the Work-Piece by Welding," Institutt for Mekanisk Teknologi, Technical University of Norway, March 7, 1968. pp. 1-64.

(70) Winterton, K. "Weldability Prediction from Steel Composition to Avoid Heat Affected Zone Cracking," Welding Journal, Vol. 40. 1961. pp. 253-s to 258-s.

(71) Yalamanchili, R. V. S. and Chu, S. U. "Stability and Oscillation Characteristics of Finite Element, Finite-Difference, and Weighted-Residuals Methods for Transient Two-Dimensional Heat Conduction in Solid." Journal of Heat Transfer, May 1973, pp. 235-239.

(72) Fujii, H. "Some Remarks on Finite Element Analysis of Time-Dependent Field Problems," Department of Computer Sciences, Kyoto Sangyo Univ., Japan.

(73) Mizikar, Eugene A. "Mathematical Heat Transfer Model for Solidification of Continuously Cast Steel Slabs," Transactions of the Metallurgical Society of AIME, Volume 239, Nov. 1967, pp. 1747-1753.

(74) Moore, Michael, Phone conversation, March 1976, U.S. Steel Corporation, Pittsburgh, PA.